Nanoscale tribology: energy dissipation mechanisms in friction

Miquel Salmeron

Materials Science Division
Lawrence Berkeley National Laboratory
University of California, Berkeley, CA. USA

Work funded by the US Department of Energy

Collaborators:

Gang-yu Liu	
Anna Lio	
Susanne Kopta	
Xudong Xiao	
Lei Xu	
Jose Benitez	U. Sevilla
D. Frank Ogletree	
Qing Dai	
Robert Carpick	
Marius Enachescu	
R.J.A. van den Oetelaar	T.U. Eindhoven
Esther Barrena	CSIC Madrid
Carmen Ocal	
Mark Mowery	U. Michigan
Prof. Christine Evans	

Quan Du	U.C. Berkeley
Prof. Y. Ron Shen	U.C. Berkeley
Peter Frantz	
Alex Artsukovich	
Frieder Mugele	
Quan Du	
Steve Baldelli	
Y. Ron Shen	
Huan Tang	Seagate
Jing Gui	«
Bo Persson	IFF Jülich
Silviu Zilberman	Tel-Aviv Univ.

Single asperity: the basic unit of contact mechanics

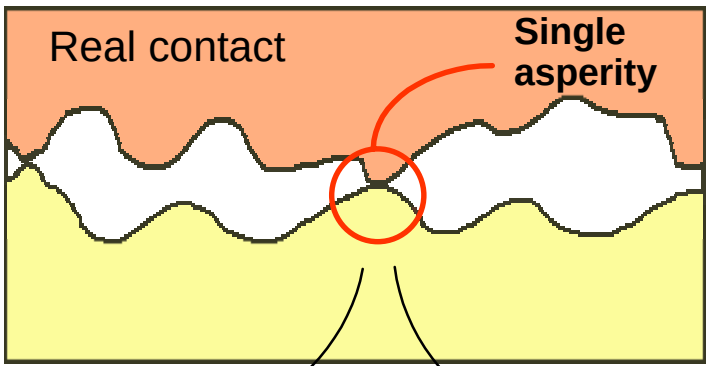

STM & AFM

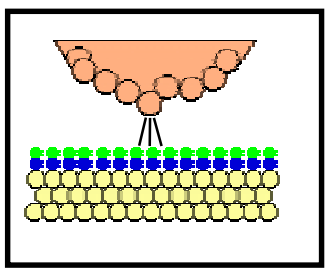

SFA

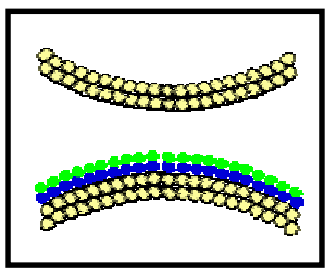

Our techniques:

SCANNING PROBE MICROSCOPY (SPM)

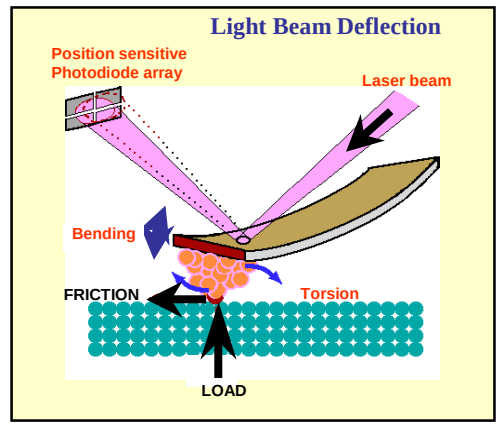

SURFACE FORCES APPARATUS (SFA)

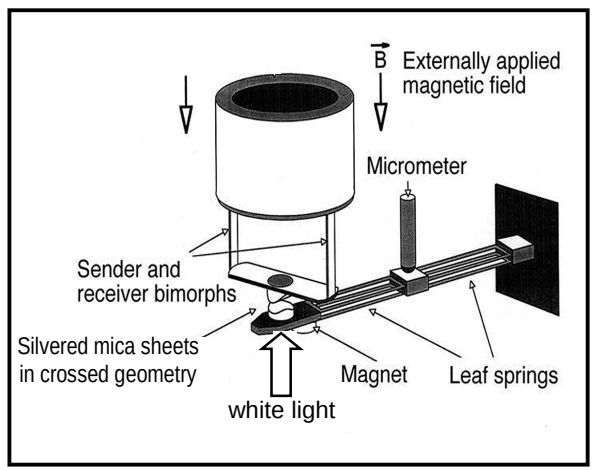

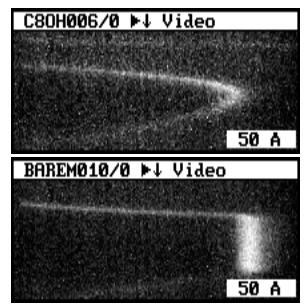

Are the predictions of classical contact mechanics valid at the nanometer scale?

Predictions from continuum mechanics (JKR and DMT limits)

JKR limit

Large μ (> 5)

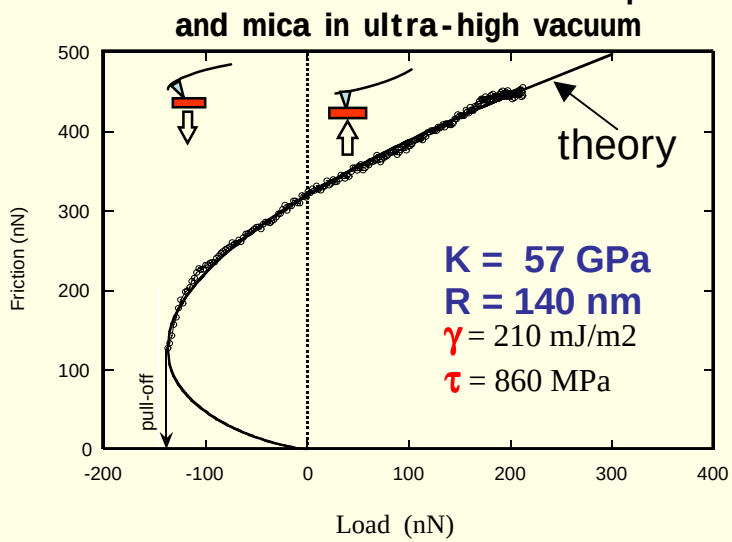

$$A = \pi \frac{R^{2/3}}{K^{2/3}} \left(L + 3\pi\gamma R + \sqrt{6\pi\gamma RL + (3\pi\gamma R)^2} \right)^{2/3}$$

Tabor parameter

$$\mu = \left(\frac{16R\gamma^2}{9K^2 z_0^3} \right)^{1/3}$$

Yes, down to nm dimensions !

DMT limit

Small μ (< 0.1)

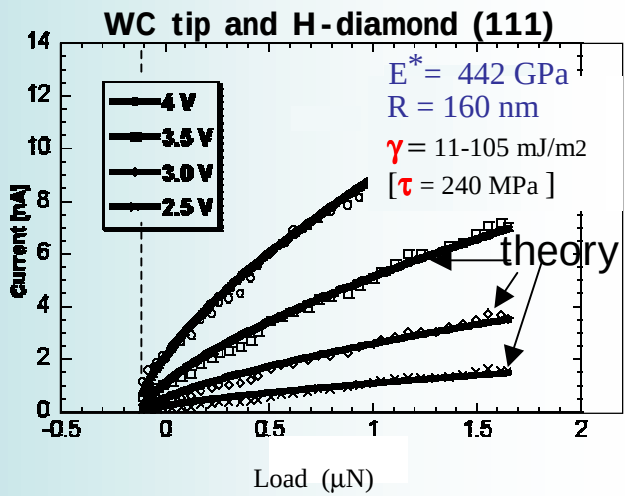

$$A = \pi \frac{R^{2/3}}{K^{2/3}} (L + 2\pi\gamma R)^{2/3}$$

Amonton's Law: $F = \mu \times L$

The linear dependence observed in macroscopic contacts is the result of multiple asperities

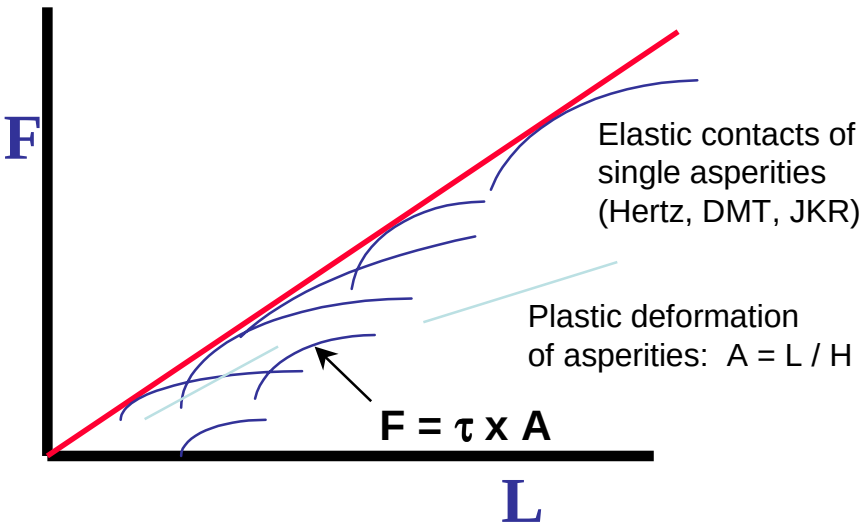

Friction vs Load curves resulting from incremental opening of new energy dissipation mechanisms

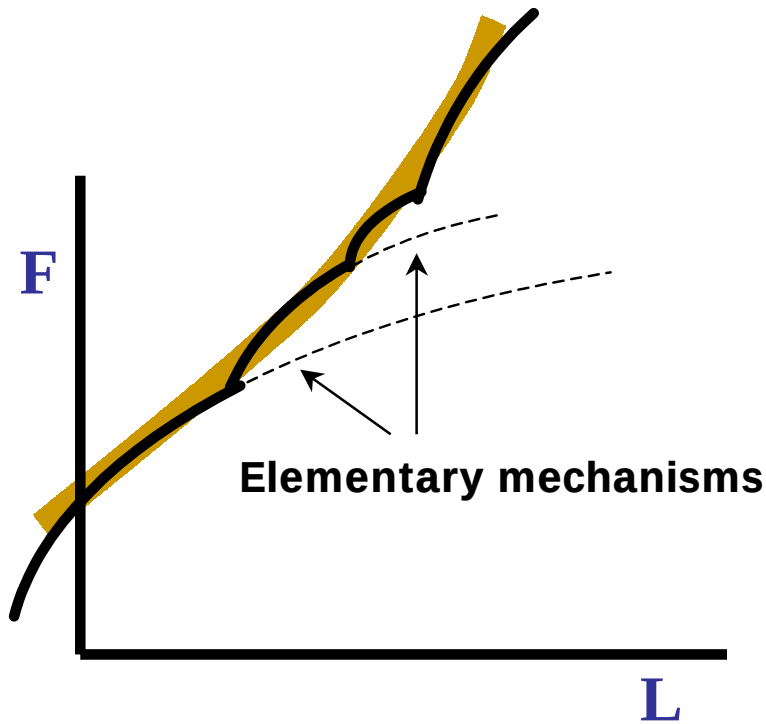

Linearity between F and L arises as a result of:

a) Plastic deformation (Bowden & Tabor)
b) Integration of elastic deformation of multiple asperities (Greenwood & Williamson)

Elementary energy dissipation processes:

	Characteristic time
1. Electronic contributions: electron hole-pairs, surface resistivity, electron wind, ...	t ~ fsec
2. Phonons	t ~ psec
3. Viscoelastic effects in lubricant layers	t ~ sec
4. Defect generation: surface point defects, dislocations	t ~ ∞

Friction and wear in a model system: alkylsilane covered mica

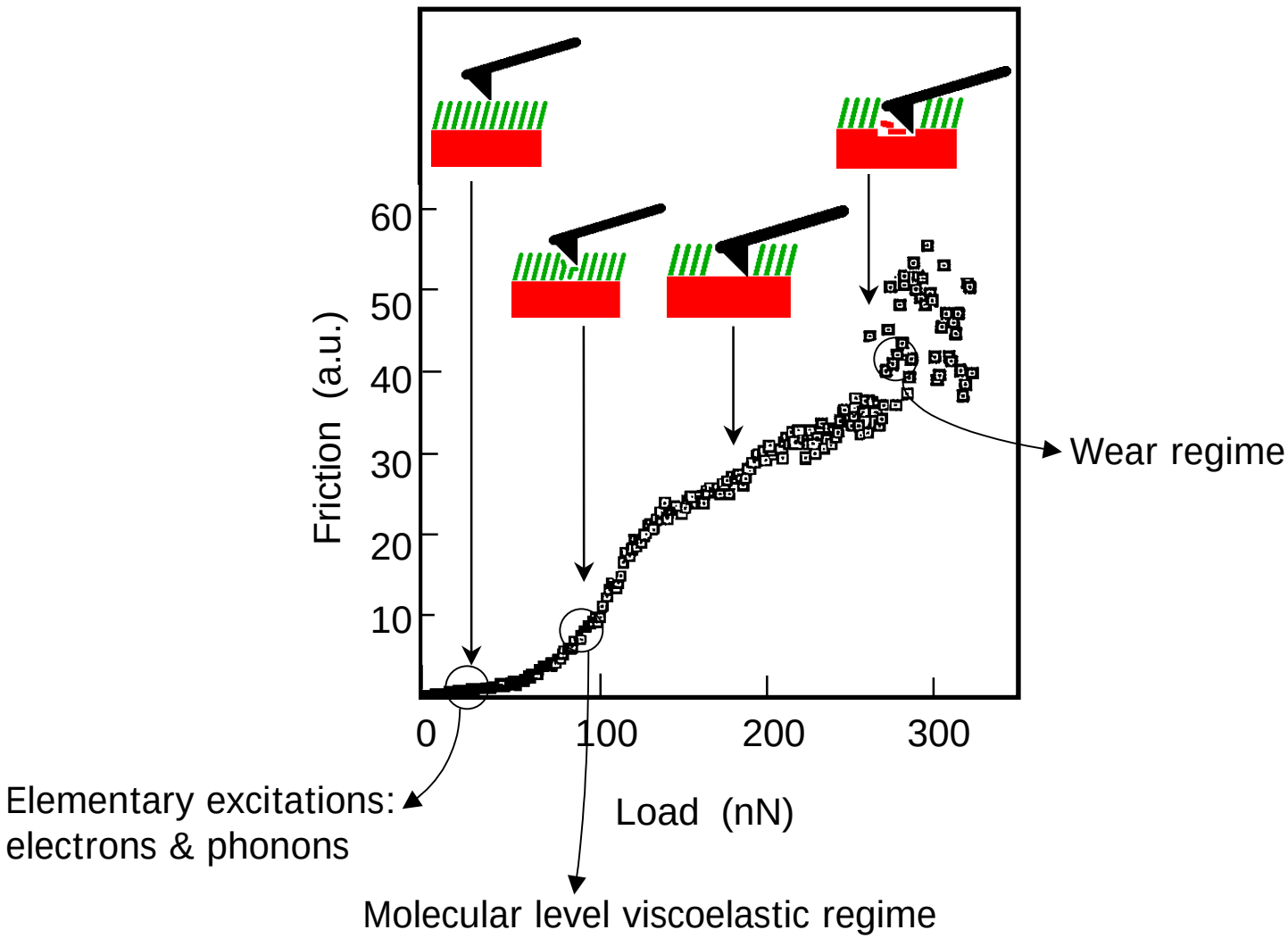

Viscoelastic energy dissipation processes in long-chain molecules

Elementary energy dissipating processes:

Terminal gauche deformations

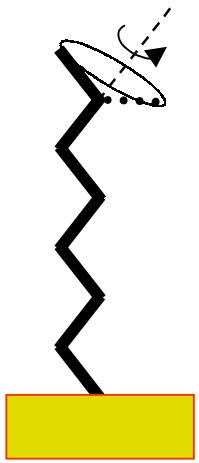

Easiest to produce because terminal groups have few steric constrains

Rigid chain tilts

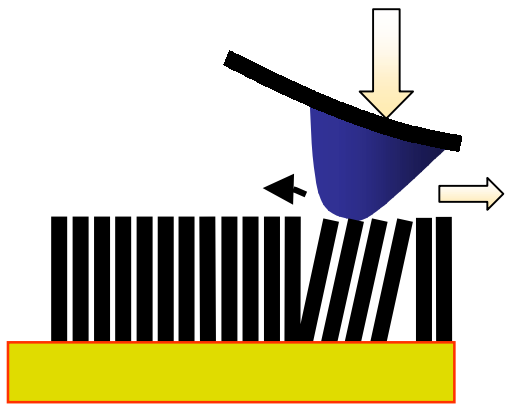

Most favorable deformation due to strong chain-chain attractive forces and steric constrains

Internal gauche deformations

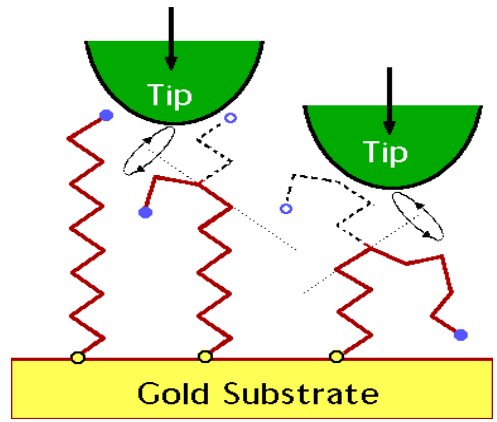

Most difficult to produce in compact films due to steric constrains

1. Sum Frequency Generation reveals molecular structure at the buried interface

Deformation of CH_3 terminal group probed with SFG

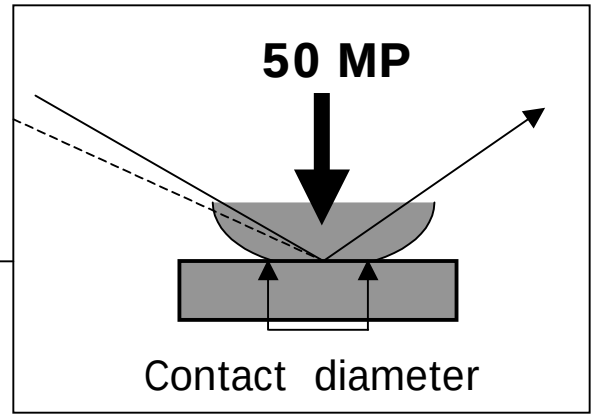

Octadecylsilanes on glass

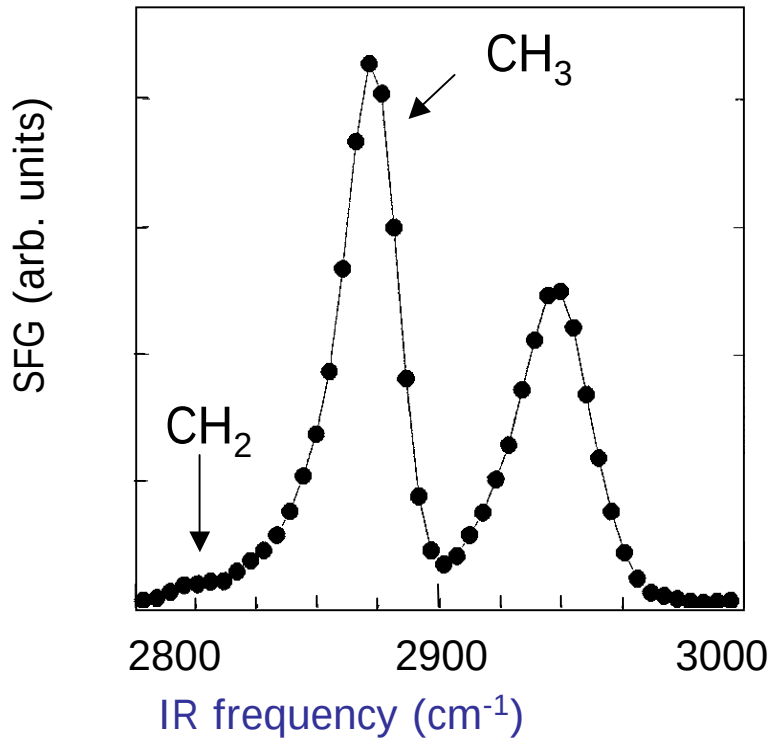

Intensity of CH_3 stretch mode under 50 MP pressure as a function of position

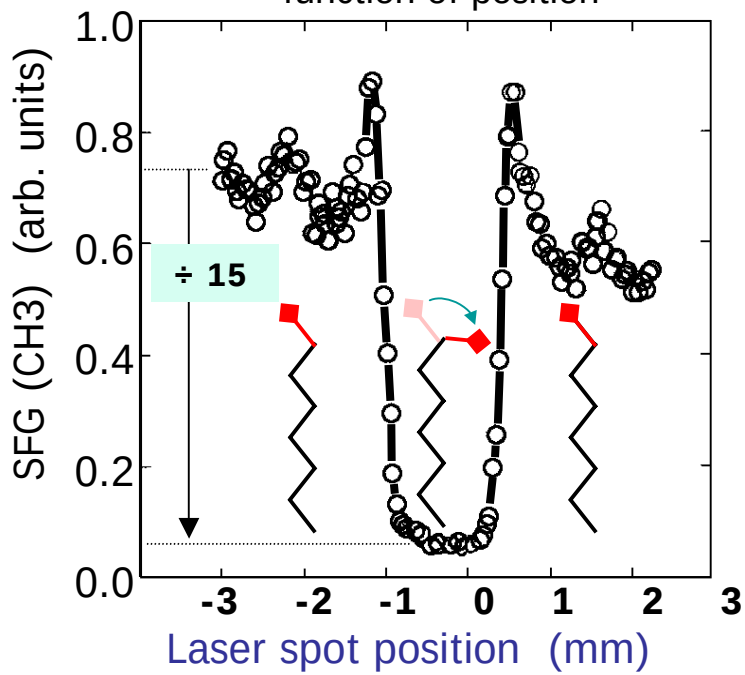

Phys. Rev. B 51, 7456 (1995)

Molecular dynamics simulations by J. Harrison et al. predict formation of terminal gauche defects under pressure

Diamond(111)

C13 alkane

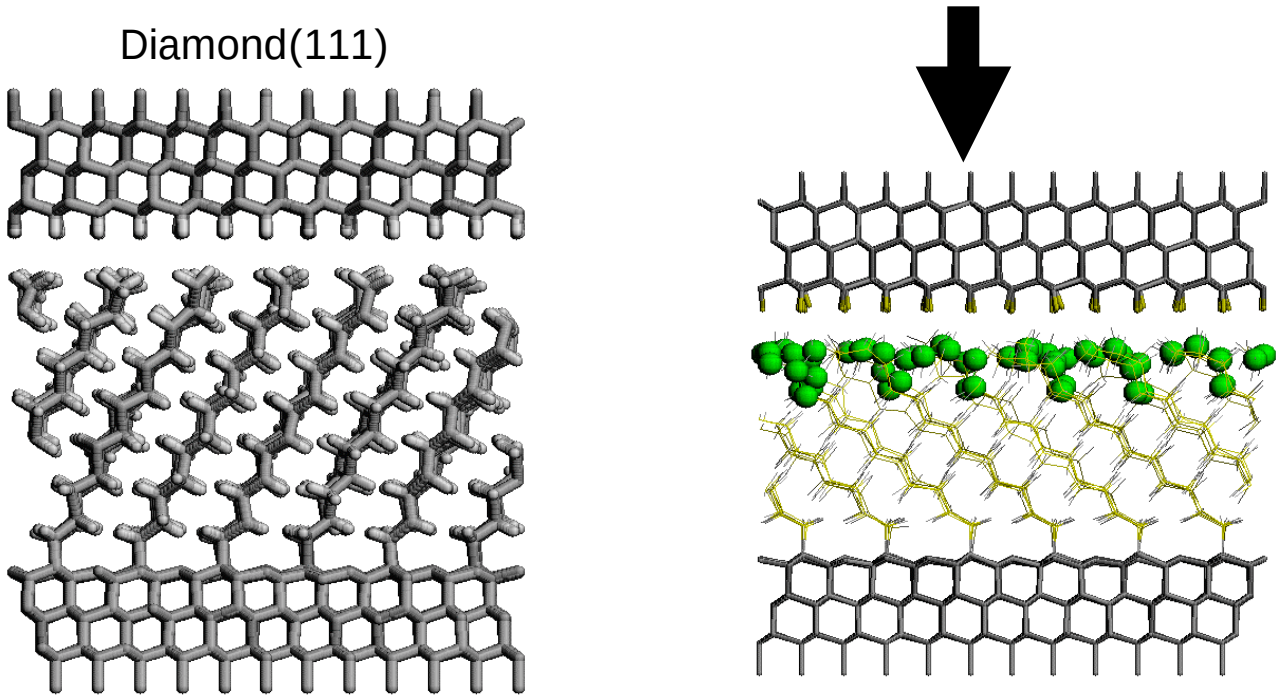

Terminal gauche defects

From: A.B. Tutein, S.J. Stuart and J.A. Harrison. **Langmuir** 16, 291 (2000)

Indentation and displacement of thiols on Au(111) by sharp AFM tips

Low load

2D Fourier transforms

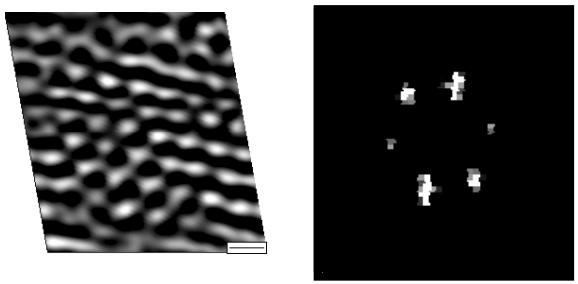

$\sqrt{3}\times\sqrt{3}\,\mathbf{R}30^{\mathbf{o}}$

High load

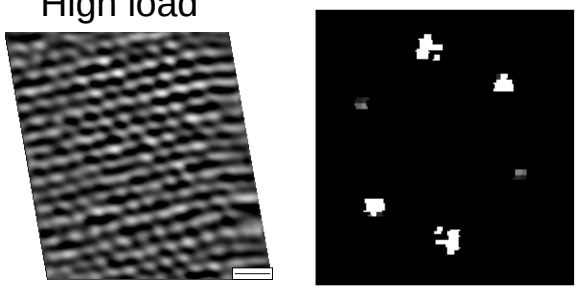

1×1

Low load

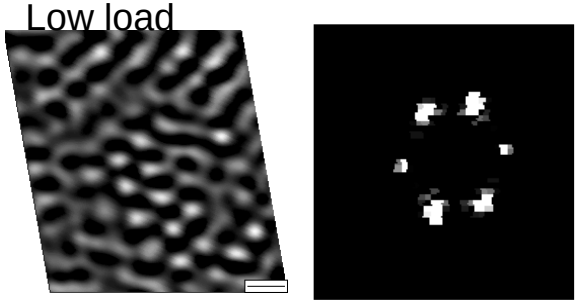

$\sqrt{3}\times\sqrt{3}\,\mathbf{R}30^{\mathbf{o}}$

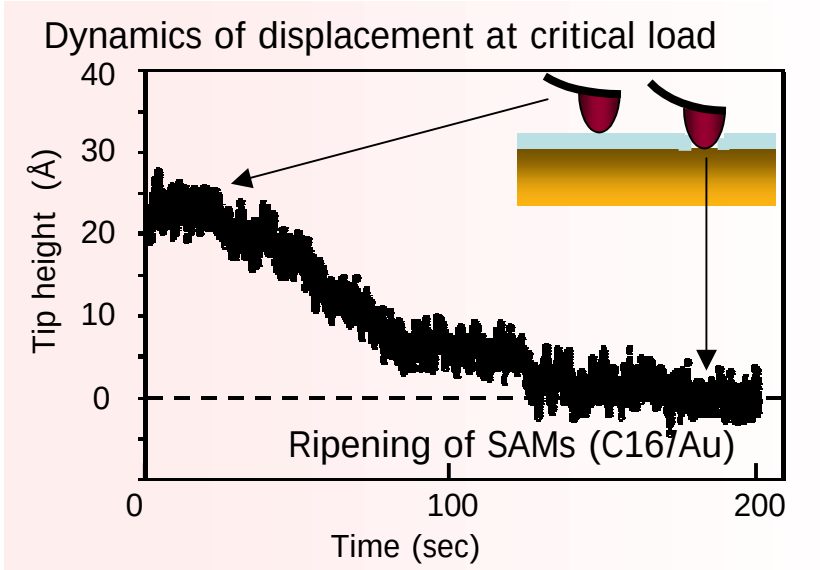

Pressure for tip penetration changes with time due to ripening

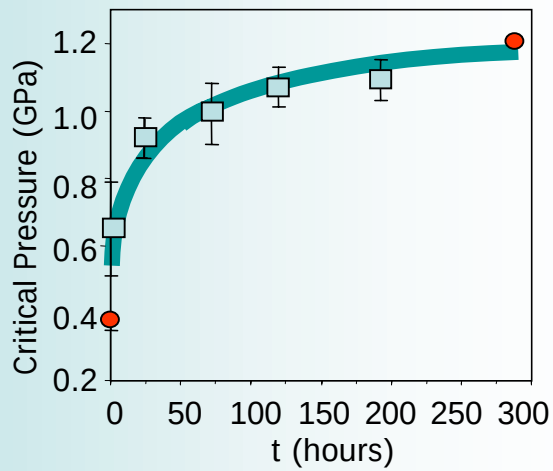

Langmuir 9, 3600 (1993); **Langmuir** 10, 367 (1994); **J. Phys. Chem. B** 101, 4767 (1997); **J. Chem. Phys.** 111, 9797 (1999)

Friction and structure of alkane-chain SAMs under pressure

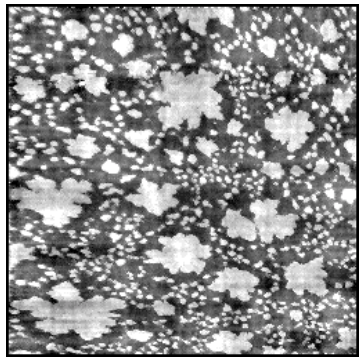

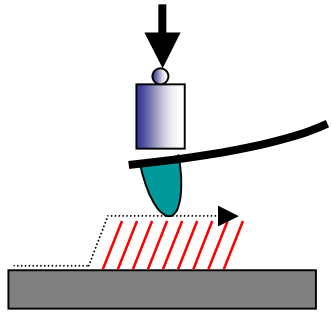

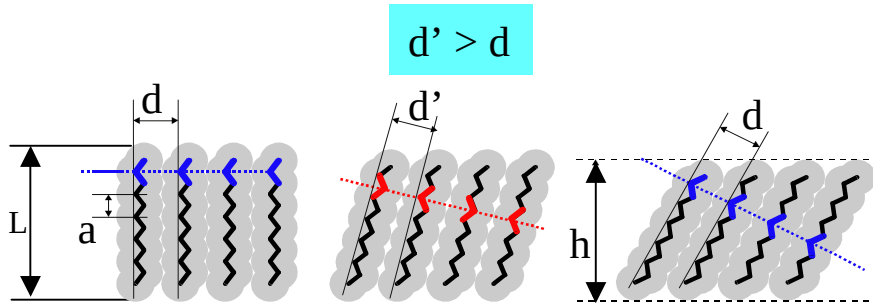

C12 silanes on mica

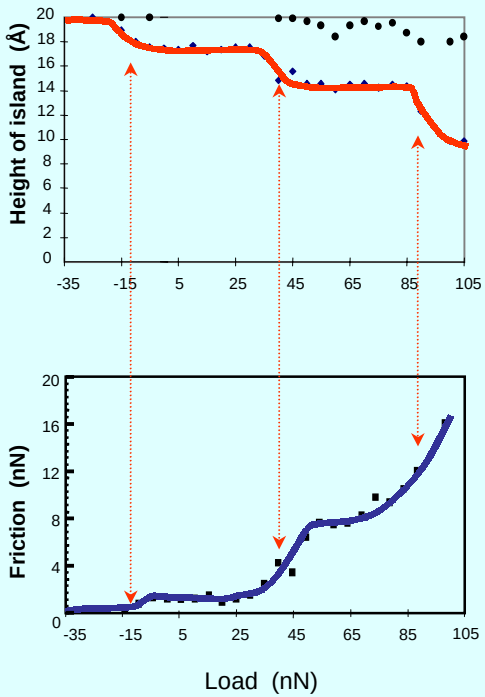

C16 thiols on gold

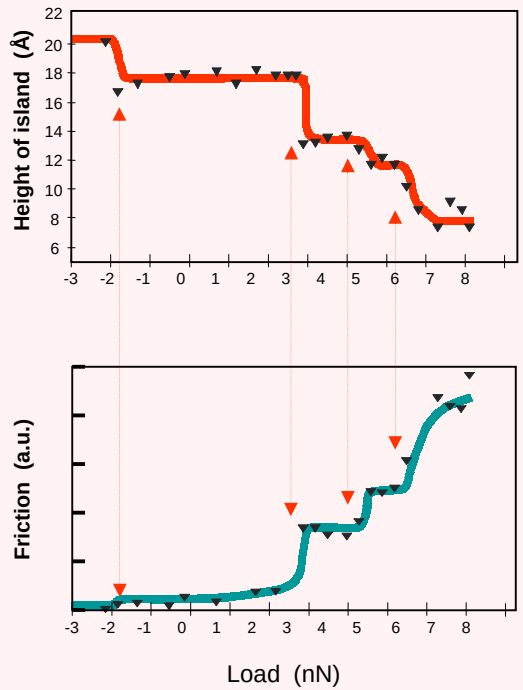

C16 amines on mica

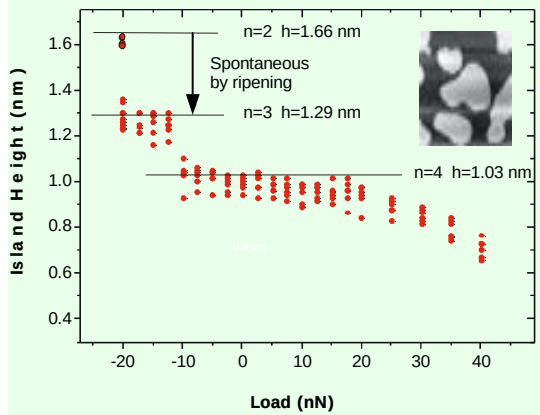

Film height in the space filling model (weak substrate binding)

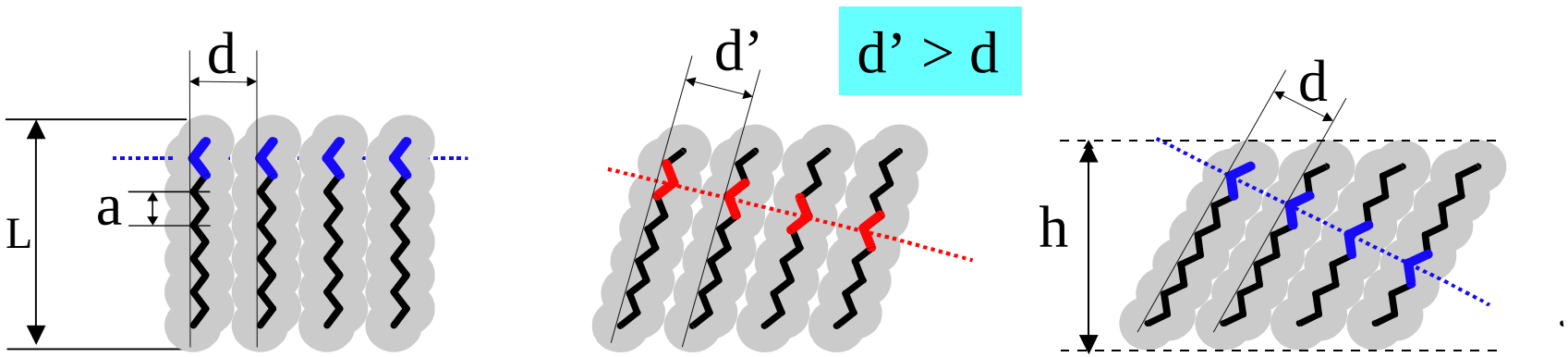

n	calculated relative height $\frac{h}{L}=\left[1+\left(\frac{na}{d}\right)^2\right]^{-1/2}$	measured relative height of the layer above mica substrate in Å		
		C12	C16	C18
0	1	0.985 ± 0.025	1 ± 0.020	1 ±0.019
1	0.883	0.860 ± 0.025	0.880 ± 0.020	0.888 ± 0.019
2	0.685	0.725 ± 0.025	0.688 ± 0.028	0.693 ± 0.026
3	0.531	0.590 ± 0.025	0.568 ± 0.020	0.537 ± 0.019
4	0.425	0.450 ± 0.025	0.468 ± 0.020	—

Film height in the space filling model (strong substrate binding)

Two tilt directions need be considered:

$$\tan\theta_X = \frac{n\,a}{d_X}, \quad n = 0,\ 0.5,\ 1,\ 1.5,\ 2\ \ldots$$

$$\tan\theta_Y = \frac{m\,a}{d_Y}, \quad \frac{m}{2} = 0,\ 0.5,\ 1,\ 1.5,\ 2\ \ldots$$

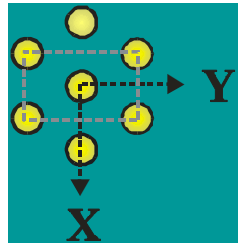

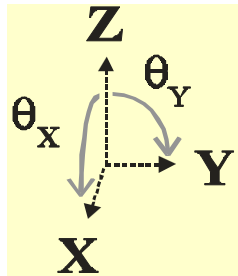

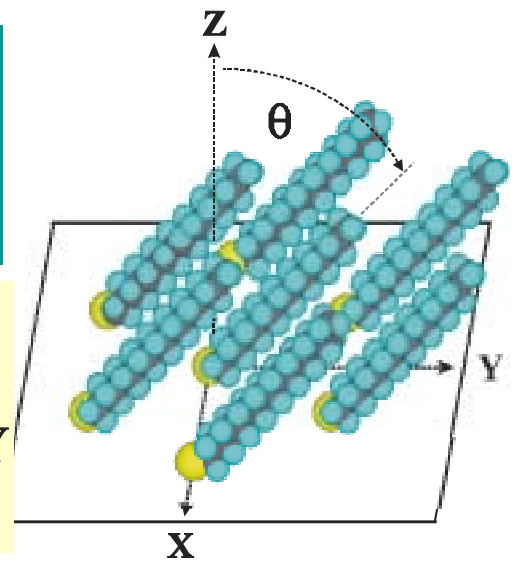

Experimental	1D model			2D model			
Height (Å)	n	α	Height (Å)	n	m/2	α	Height (Å)
19.7± 0.4	1	30º	20.7	0	1	35º	19.6
18± 1			. . .	1	1	43º	17.6
				1	1.5	50º	15.7
. . .	2	49º	15.6				. . .
14.2± 0.5			. . .	2	1	55º	13.9
12± 1	3	60º	11.9	2.5	1	59º	12.2

Molecular tilt is not uniform. It starts at the island edges because the concentration of vacancies increases towards the periphery

L = 5-20 nN

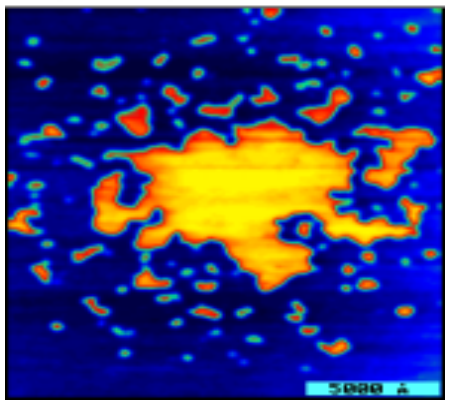

L ~ 40 nN

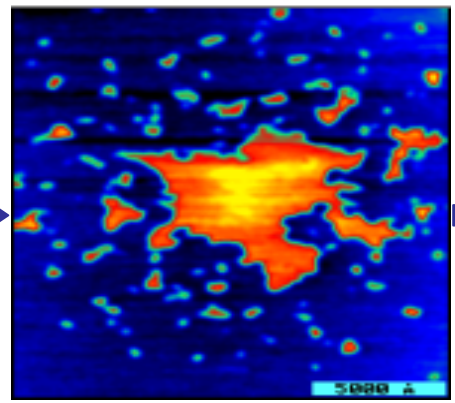

L = 45 - 80 nN

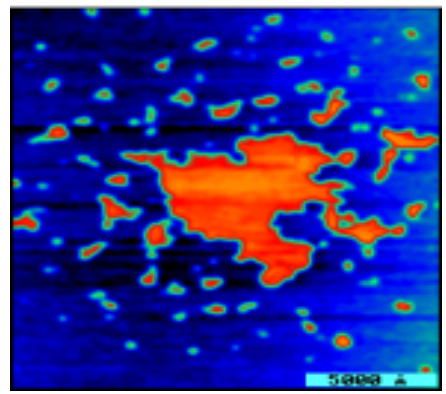

n^{th} plateau

Center= n^{th} plateau
Periphery = n^{th}+1 plateau

n^{th}+1 plateau

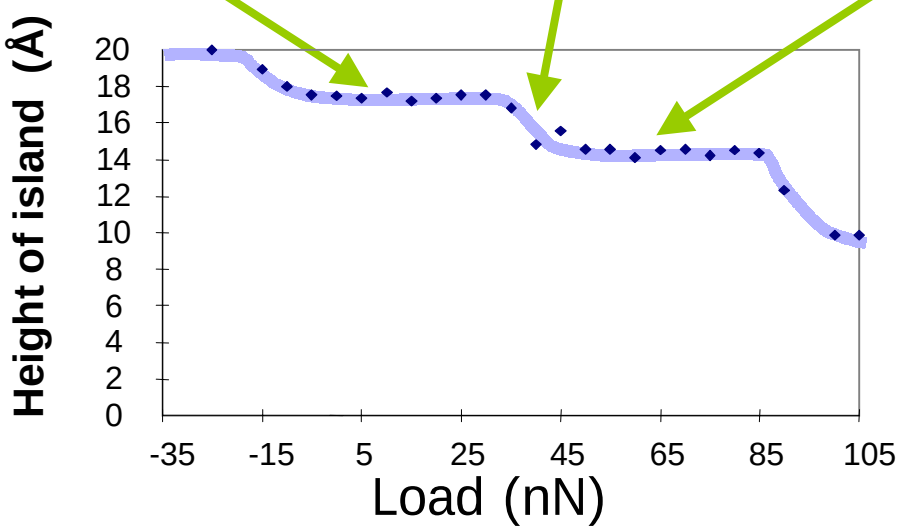

Molecular density increases from the edge to center due to slow diffusion and aggregation processes

Pressure-induced tilt is reversible

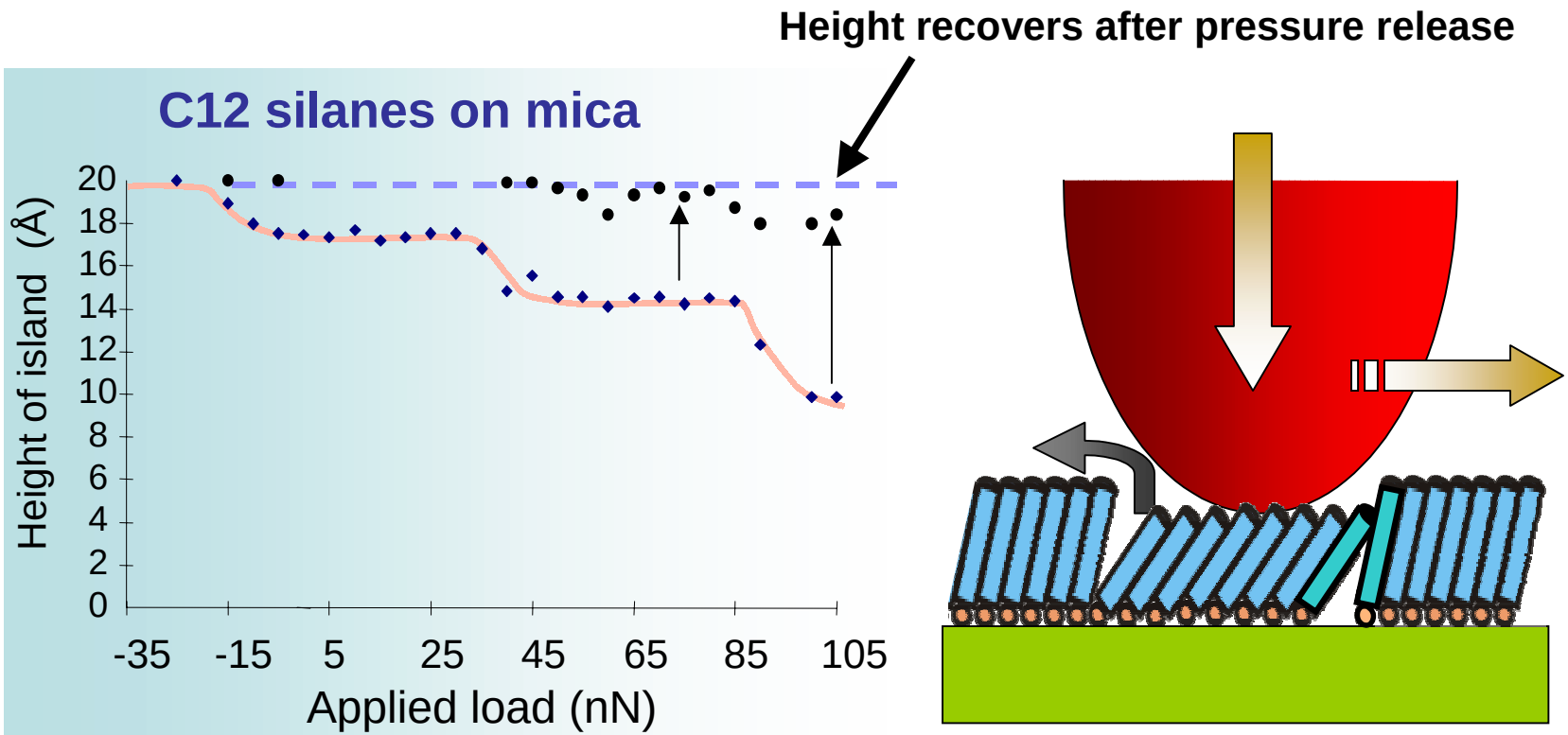

Are the tilted phases stable only under the load of the tip ?

Geometrical constrains for tilted phases

Chain–locking conditions:

$$\begin{cases} \tan\theta_X = \dfrac{n\,a}{d_X}, & n = 0,\ 0.5,\ 1,\ 1.5,\ 2\ \ldots \\ \tan\theta_Y = \dfrac{m\,a}{d_Y}, & \dfrac{m}{2} = 0,\ 0.5,\ 1,\ 1.5,\ 2\ \ldots \end{cases}$$

Commensurability conditions:

$$\begin{cases} \cos\theta_x = d_x / n' L_x \\ \cos\theta_y = d_y / m' L_y \end{cases}$$

Constrain # 1: chain-chain matching

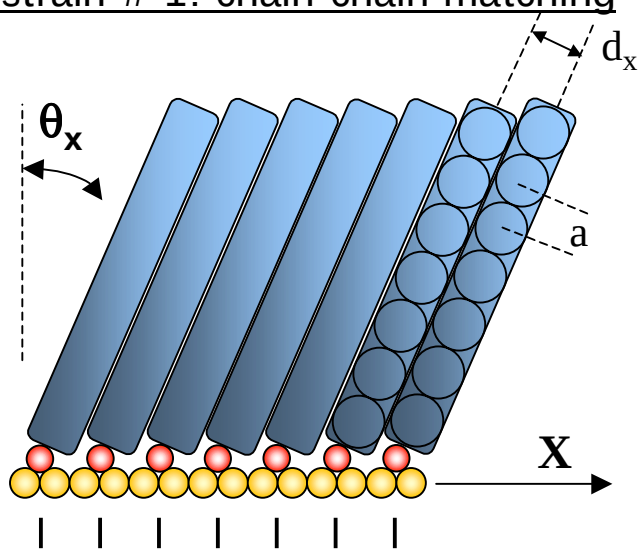

Cahin locking + Commensurate

Constrain # 2: substrate lattice matching

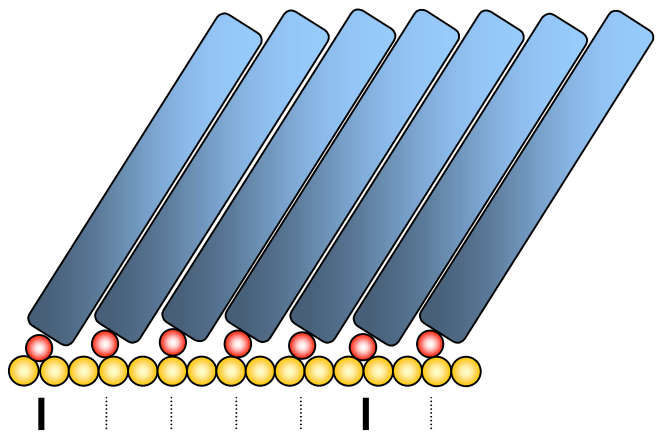

Chain locking + Incommensurate

On gold substrates alkythiols can produce metastable tilted phases if both chain and substrate lattice matching conditions are met

C16 thiols on gold

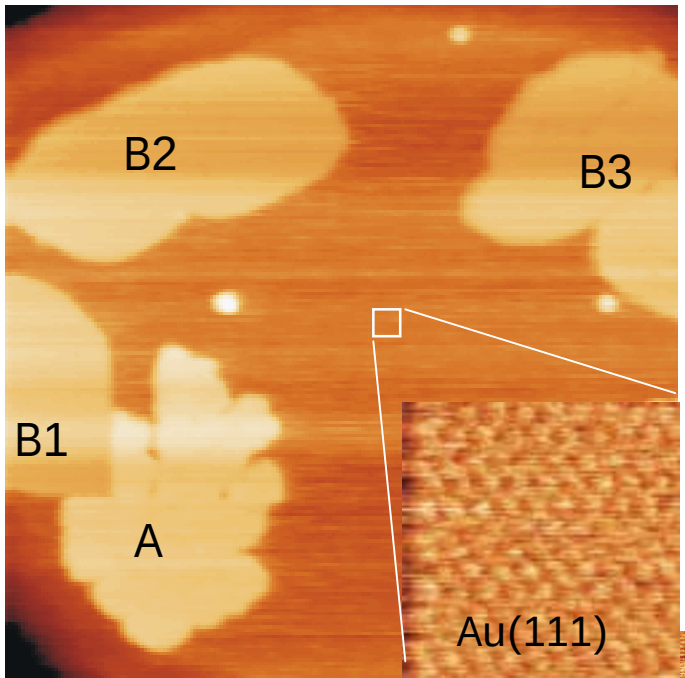

n = 0
m / 2 = 1

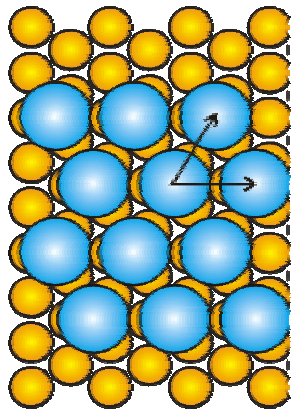

A: (√3x√3)R30°

n = 1
m / 2 = 1.5

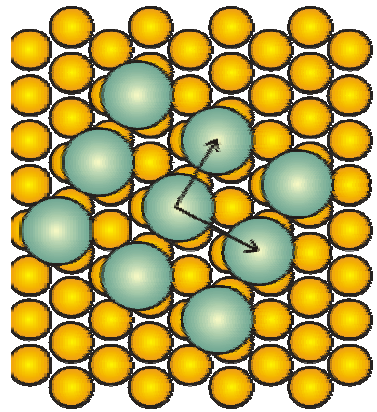

B: (2x√3)rect

Three orientational B- type domains:

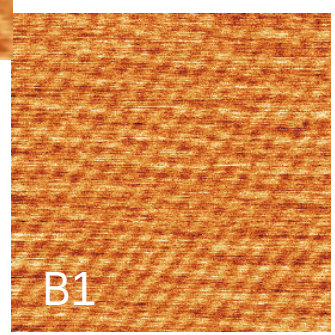

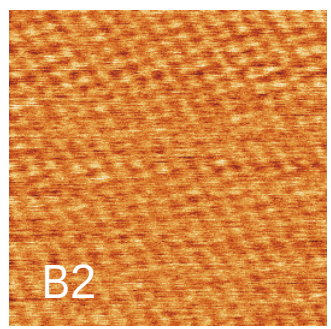

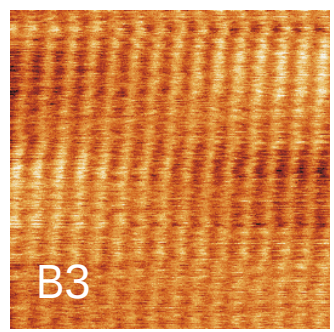

Tilted phases exhibit similar friction (at the same load)

Thiols on gold

Topography **Friction**

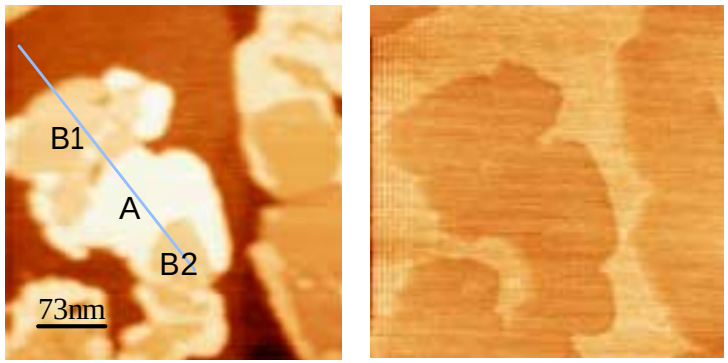

Line profile A

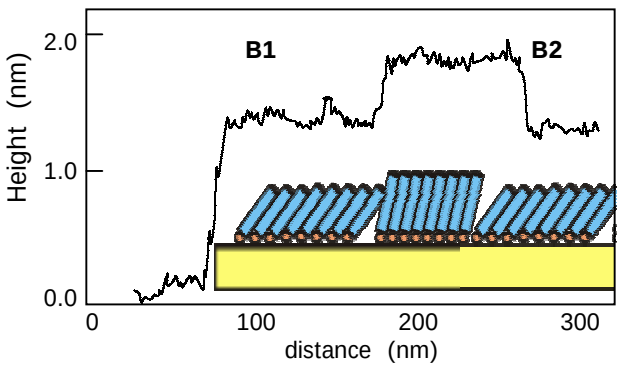

Amines on mica

Topography **Friction**

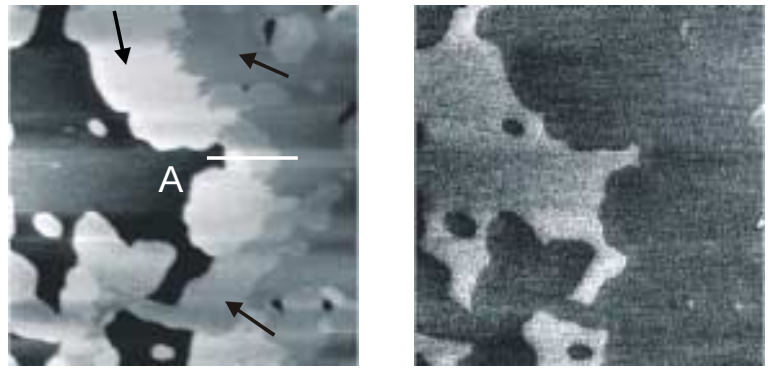

Line profile A

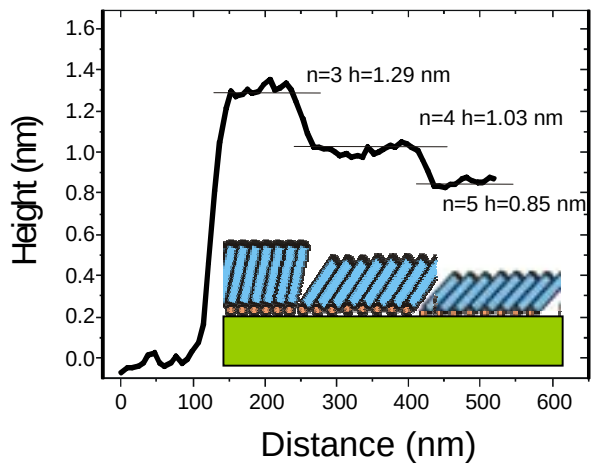

Stable and metastable phases: C18 and C22

Metastable phases can be transformed into stable ones by tip pressure

Imaging load = 0 nN

C18

C22

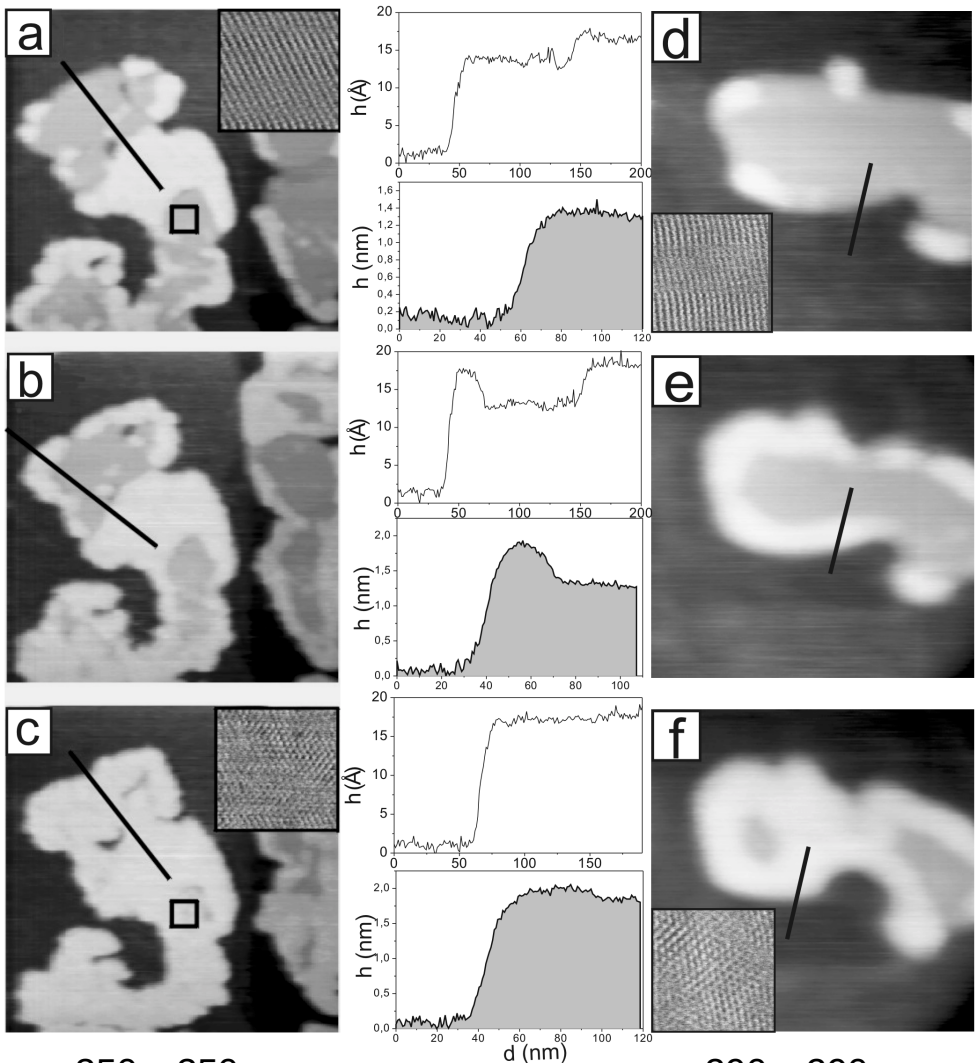

350 x 350 nm

290 x 290 nm

Applied load:

C18

0 nN

20 nN

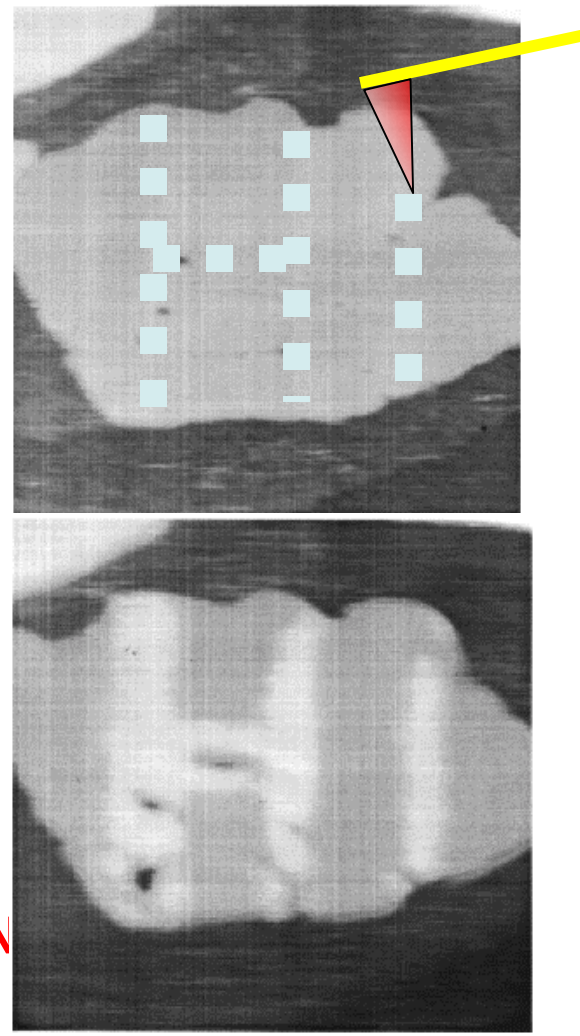

E. Barrena, C. Ocal and M. Salmeron. **J. Chem. Phys.** 114, 4210 (2001)

Cross-linking the molecules blocks tilting mechanism: SAM of alkylthiol molecules with diacetylene groups on Au(111)

Before polymerization

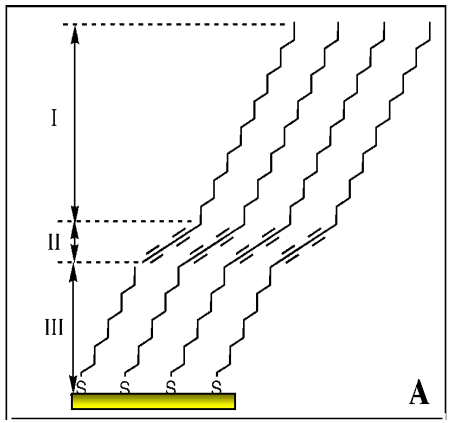

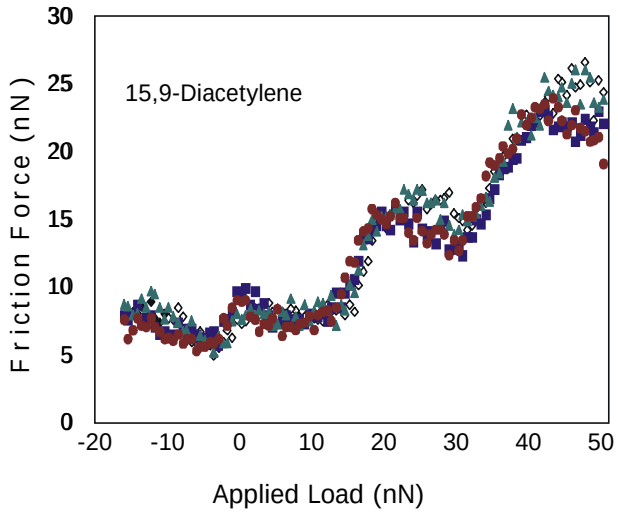

After polymerization

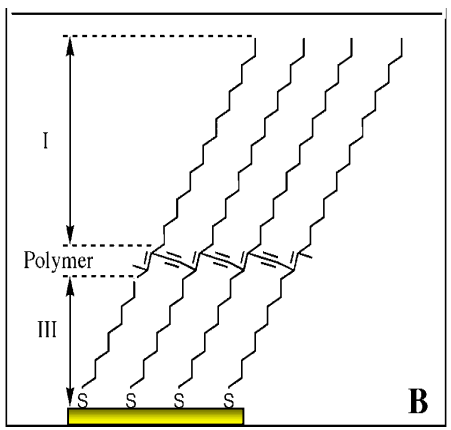

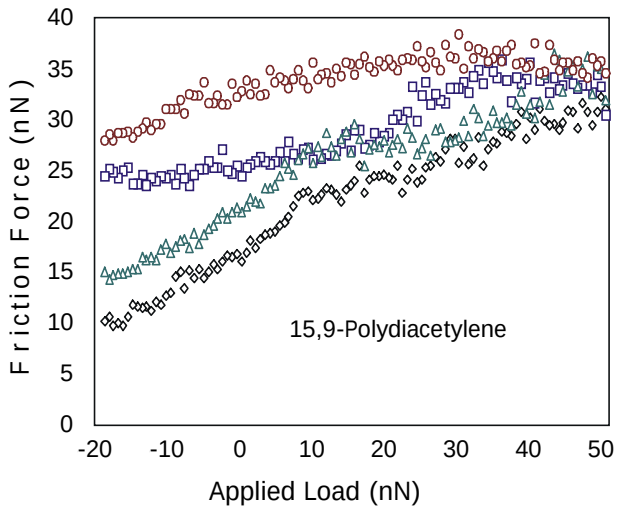

Langmuir, 15 (1999) 5118

Calculation of the van der Waals cohesive energy of alkane chain SAMs

Energy of methylene group at position *m* due to a plane of methylene units at *n* :

$$E_n^m = \sum_{|\vec{j}|=1}^{100} \frac{a}{r_{m,\vec{j}}^{\,6}}$$

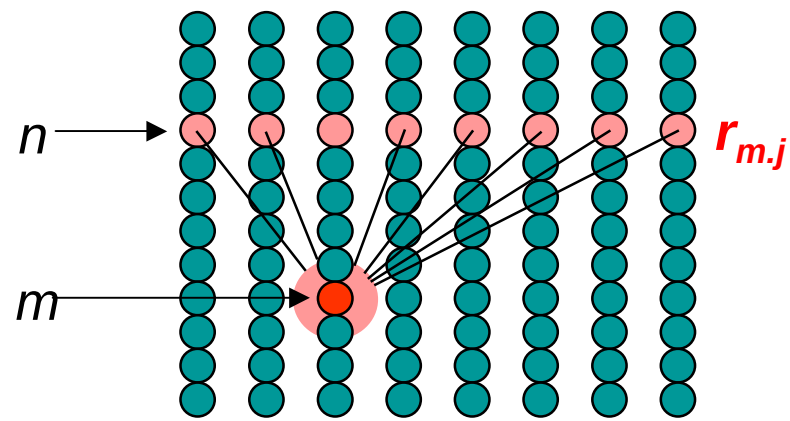

Total energy of methylene group at position *m* :

$$E_m = \sum_{n=bottom}^{top} E_n^m$$

Van der Waals coefficient ***a*** obtained from sublimation energy of N-alkanes

Total energy of monolayer film :

$$E_{total} = \frac{1}{2} \sum_{m=1}^{N} E_m$$

Trib. Lett. 10, 69 (2001)

Calculated van der Waals energy of alkyl chains as a function of tilt angle

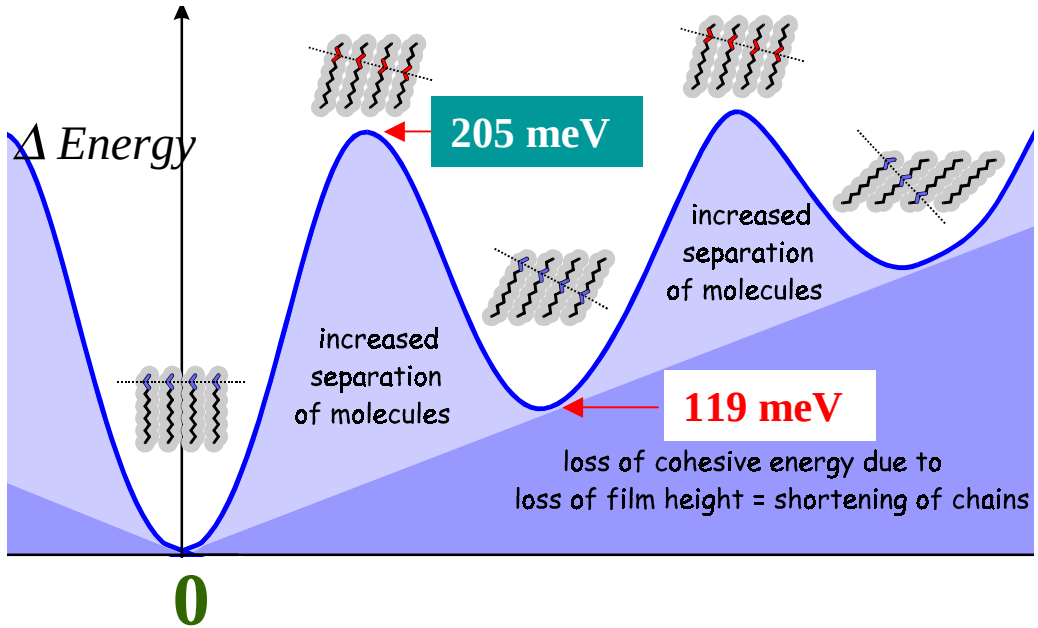

Assumption :

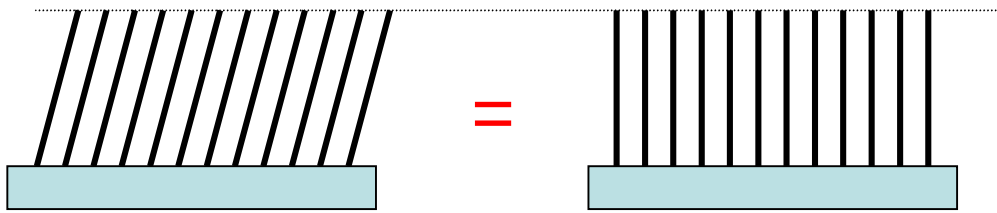

Friction force = ΔE ×(#of molec. swept per unit distance)

Contribution from internal gauche deformations can be discerned in mixed films of different chain lengths

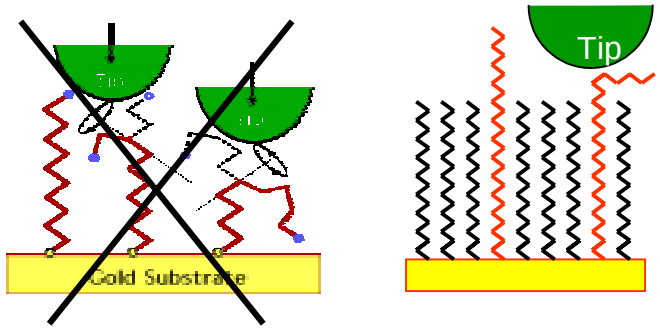

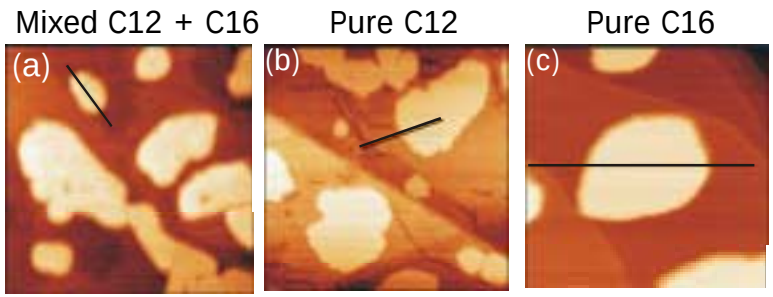

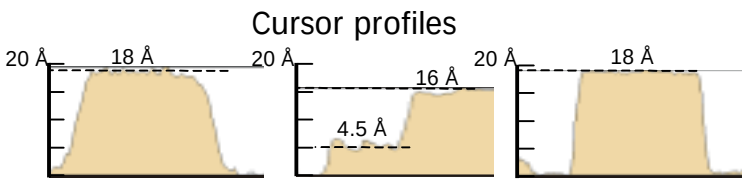

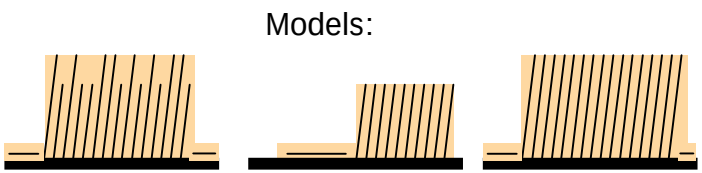

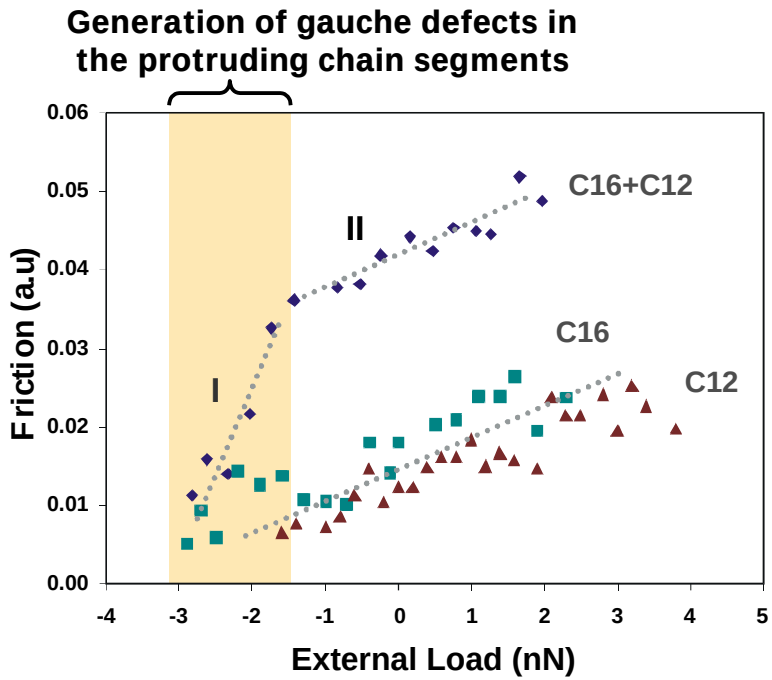

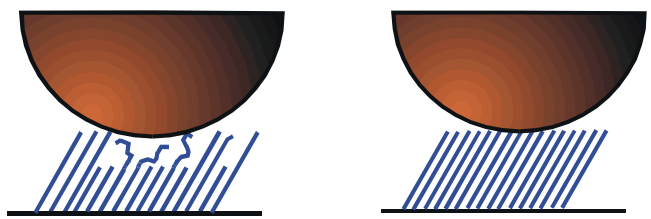

Confined liquids

The tools

1. SURFACE FORCES APPARATUS (SFA)

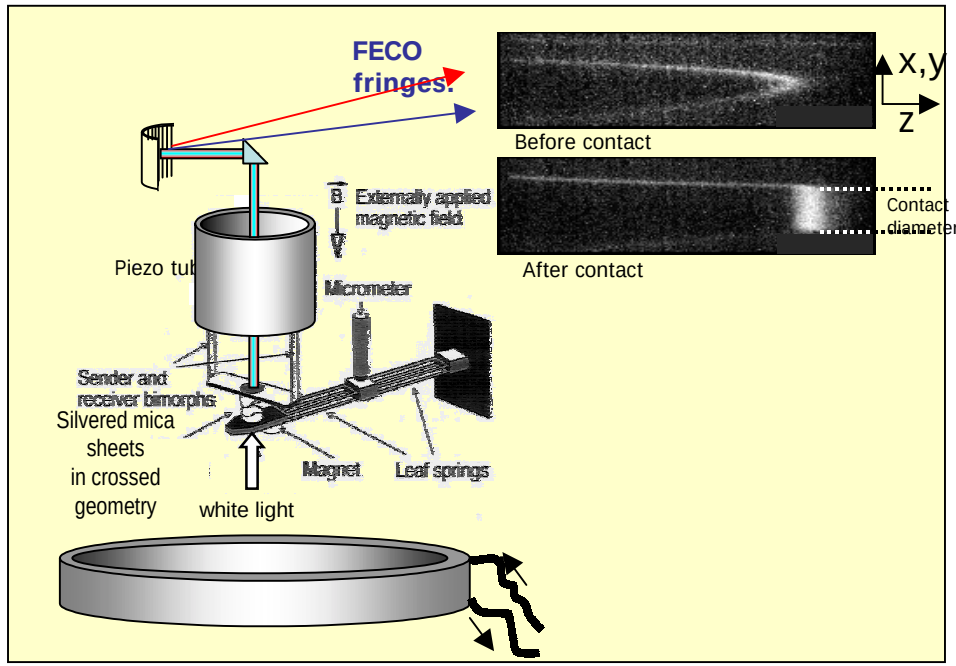

2. Non-linear optical spectroscopy: Sum Frequency Generation (SFG)

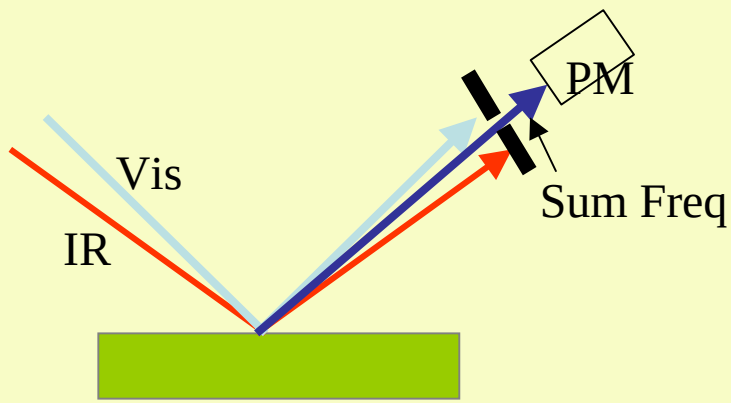

3. Scanning Polarization Force Microscopy to image liquids

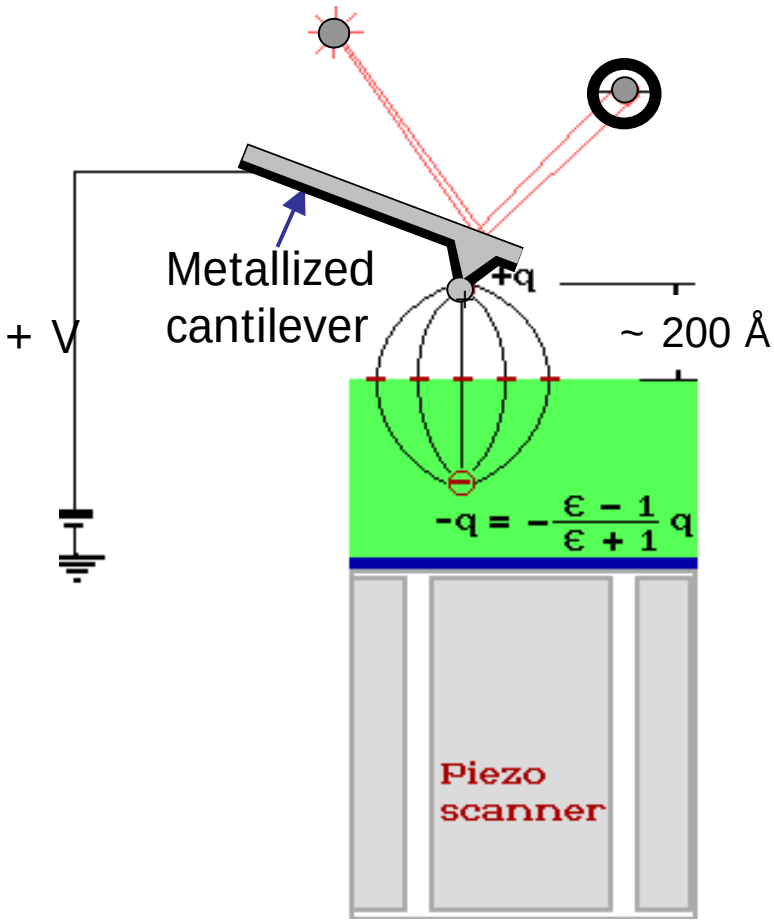

Non-contact SPFM

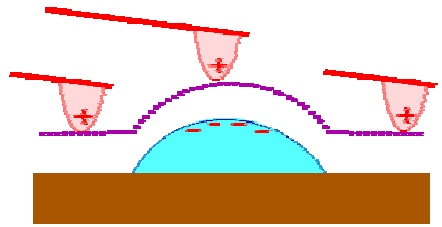

Contact Image

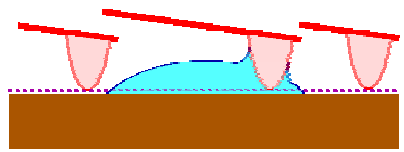

For a review on SPFM see:
L. Xu and M. Salmeron
in "**Nano-Surface Chemistry",** ed. M. Rosoff. New York: Marcel Dekker, 2001.

Adsorption of alkane-chains alcohols on mica

Contact angle measurements

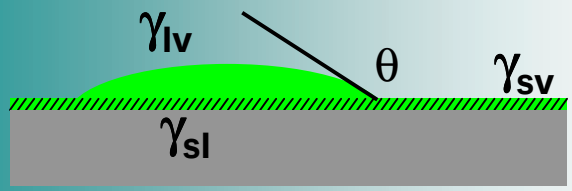

	freshly cleaved mica	silane-covered mica	silane-covered glass
C_8OH	48-50°	50°	
$C_{11}OH$	52°	50°	46°
$C_{11}H_{24}$	<5° spreads	37°	33°

Surface energies (mJ/m²): OTS: 20; $C_{11}OH$: 29; C_8OH: 27; $C_{11}H_{24}$: 25; mica: 200; ⇒ **γ (OTS-C_xOH) ≈ 1 mJ/m²)**

Sum frequency generation

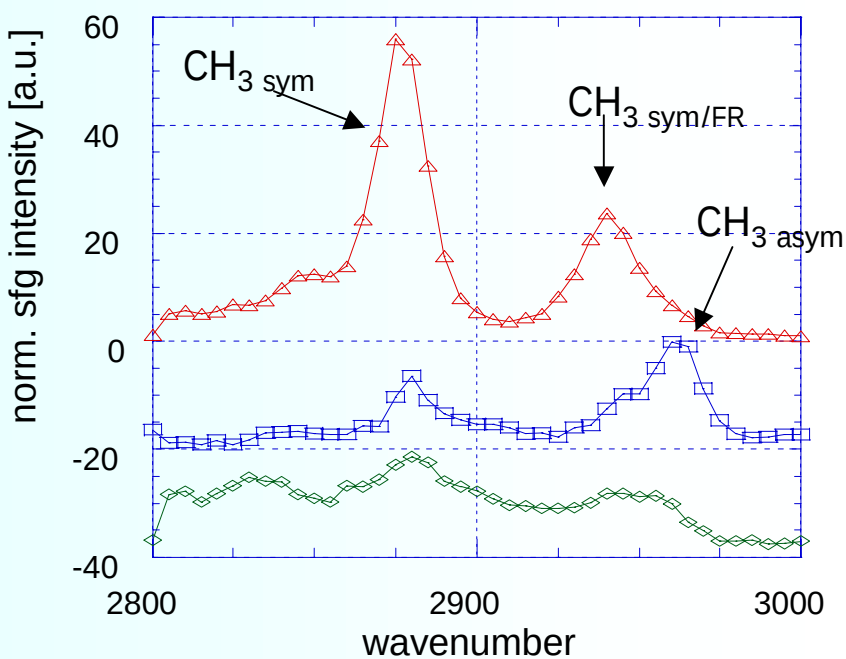

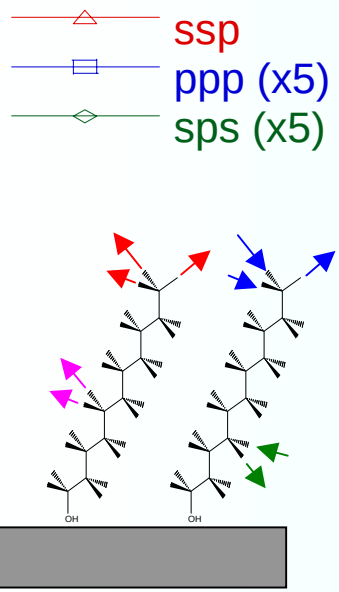

$CH_{3\ sym}$: 2870 cm^{-1}
$CH_{3\ sym/FR}$: 2940 cm^{-1}
$CH_{3\ asym}$: 2960 cm^{-1}
$CH_{2\ asym}$: 2926 cm^{-1}
$CH_{2\ sym}$: 2853 cm^{-1}

J. Phys. Chem. 104 (14), 3140 (2000).

Expulsion of octanol bilayers in the Surface Forces Apparatus

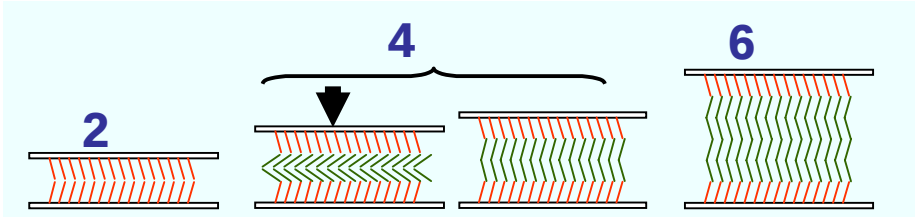

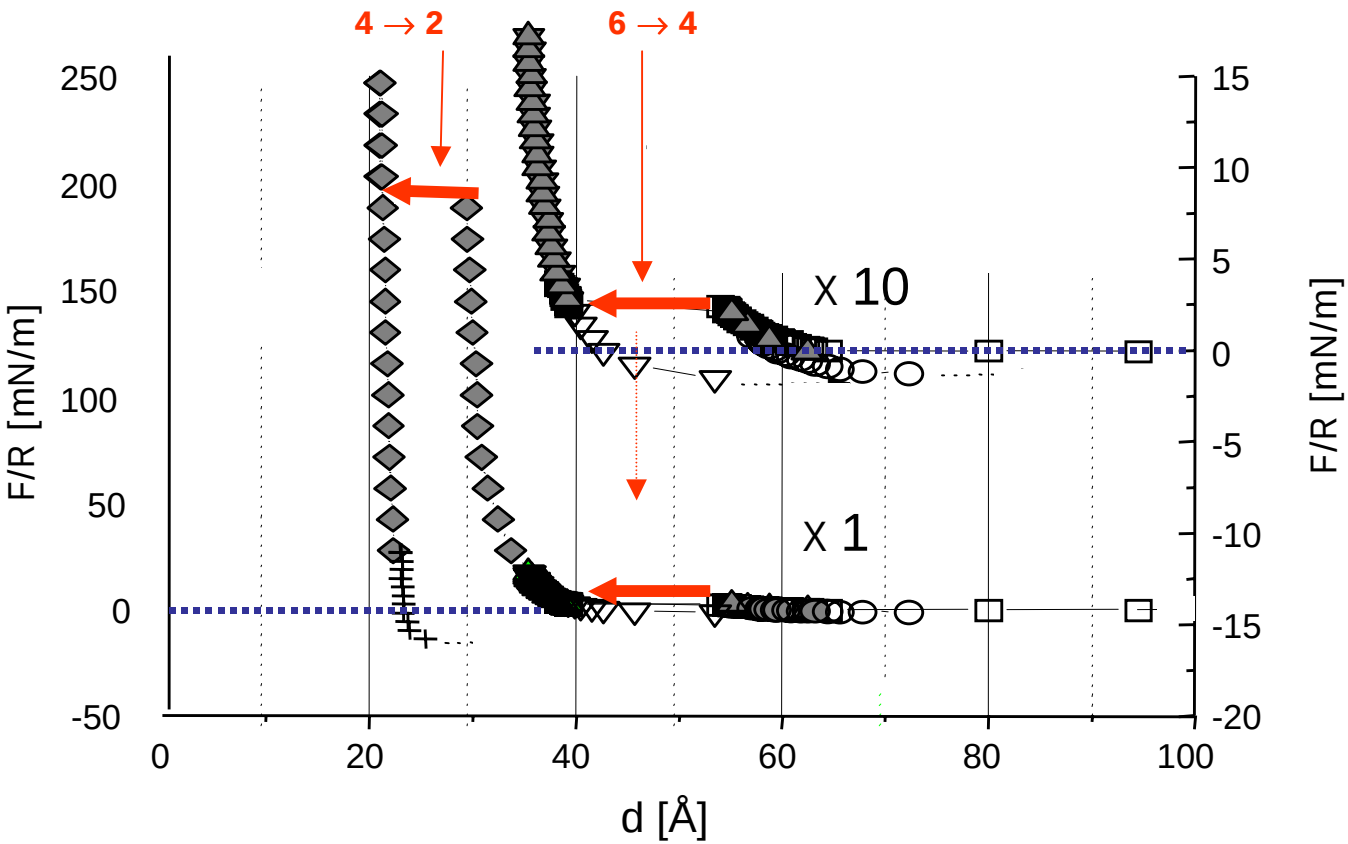

Imaging the 4 → 2 layering transition

Fabry-Perot interferometer

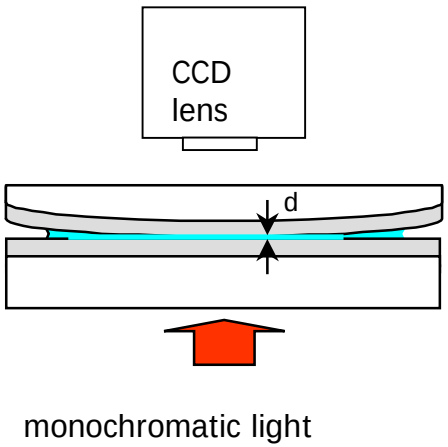

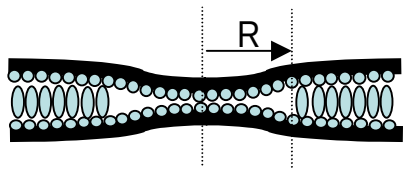

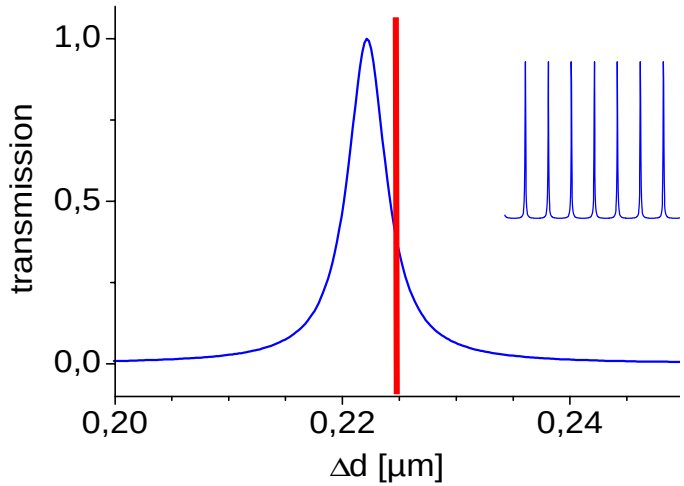

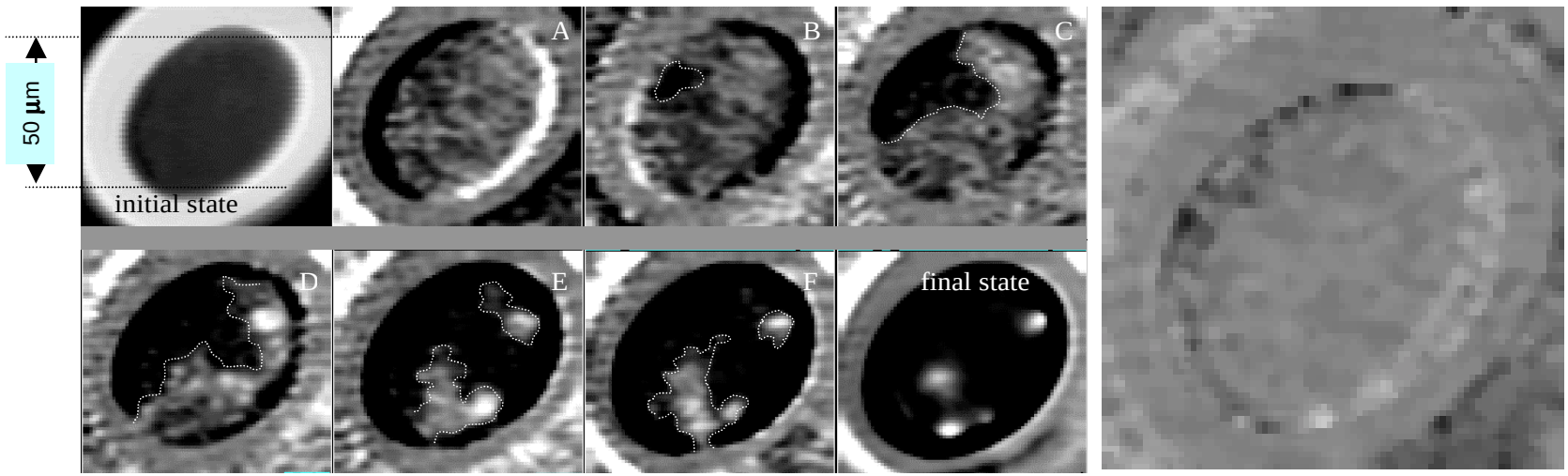

F. Mugele and M. Salmeron, **Phys. Rev. Lett.** 84 (25), 5796 (2000)

Growth of 2-D hole

Navier-Stokes equation:

$$\nabla \mathbf{v} = 0\,; \qquad \frac{\partial \mathbf{v}}{\partial t} + \cancel{\mathbf{v}(\nabla \mathbf{v})} = -\frac{1}{\rho_{2D}}\nabla p_{2D} + \cancel{\eta_{2D}\nabla^2 \mathbf{v}} - \overset{\text{friction term}}{\overline{\eta}}\mathbf{v}$$

reduces to $\nabla^2 \Phi = 0$

with $\boxed{\Phi = -\frac{p}{\rho \cdot \overline{\eta}}}$ and $\boxed{\vec{v} = \nabla \Phi}$

Off-center nucleation:

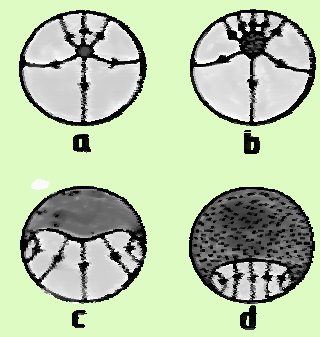

Squeeze-out time = $m\, n_a \eta A_0 / 4\pi h_0 P_{ext}$

From our data we obtain $\eta = 10^{13}\ s^{-1}$

Development of instabilities:

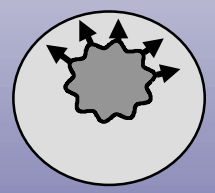

Kinetic Monte Carlo simulations:

Without line tension: fractal growth

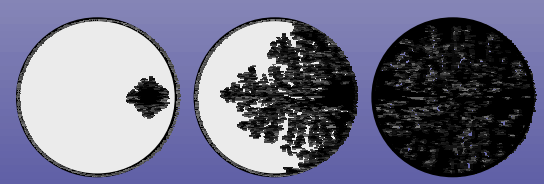

With line tension

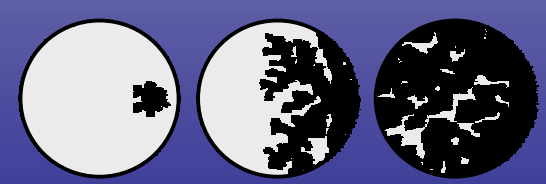

S. Zilberman, B.N.J. Persson, A. Nitzan, F. Mugele and M. Salmeron. **Phys. Rev. E**, 63, 055103(R), 2001

Evolution of trapped layers

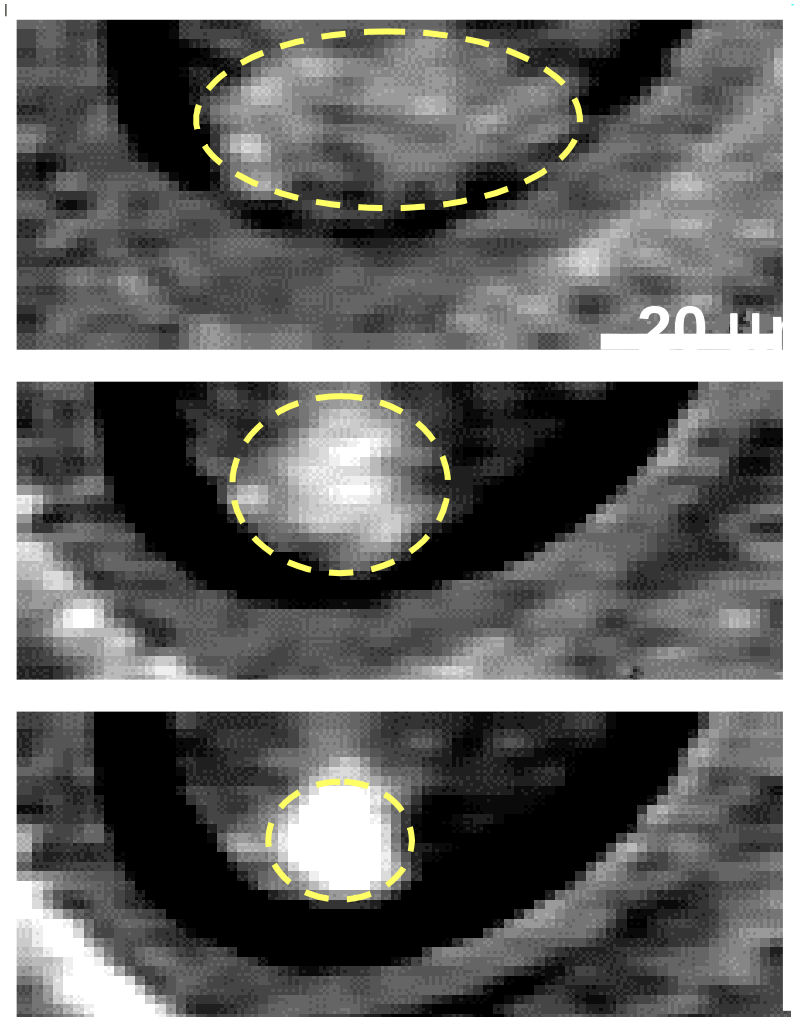

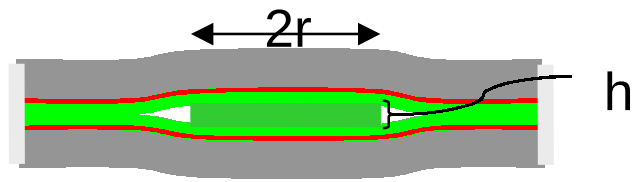

$$U(r,h)=2\gamma\pi\cdot r^2+\frac{E}{2(1-\nu^2)}\cdot r\cdot h^2$$

Surface energy of layer interfaces

Elastic energy of mica deformation

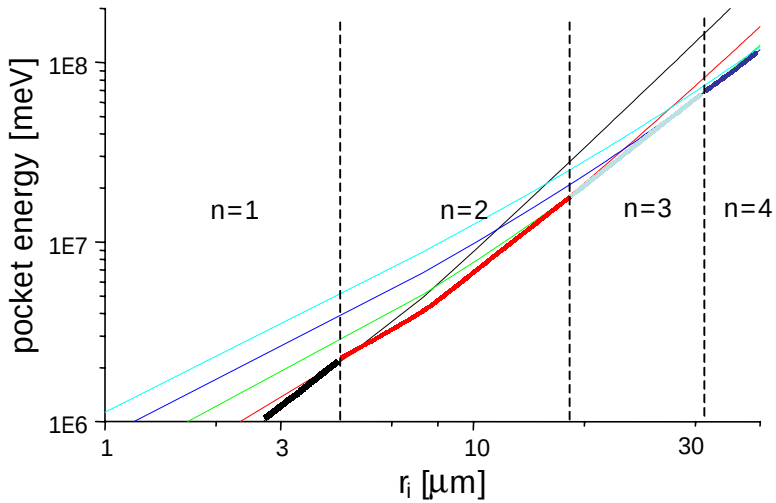

From hydrodynamic to boundary lubrication

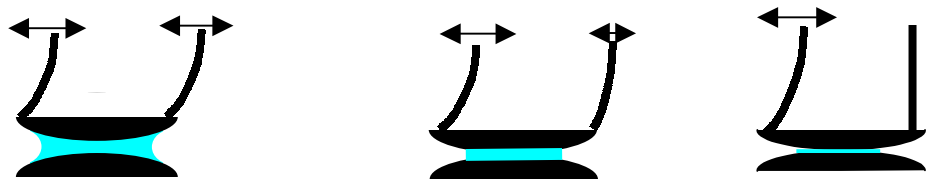

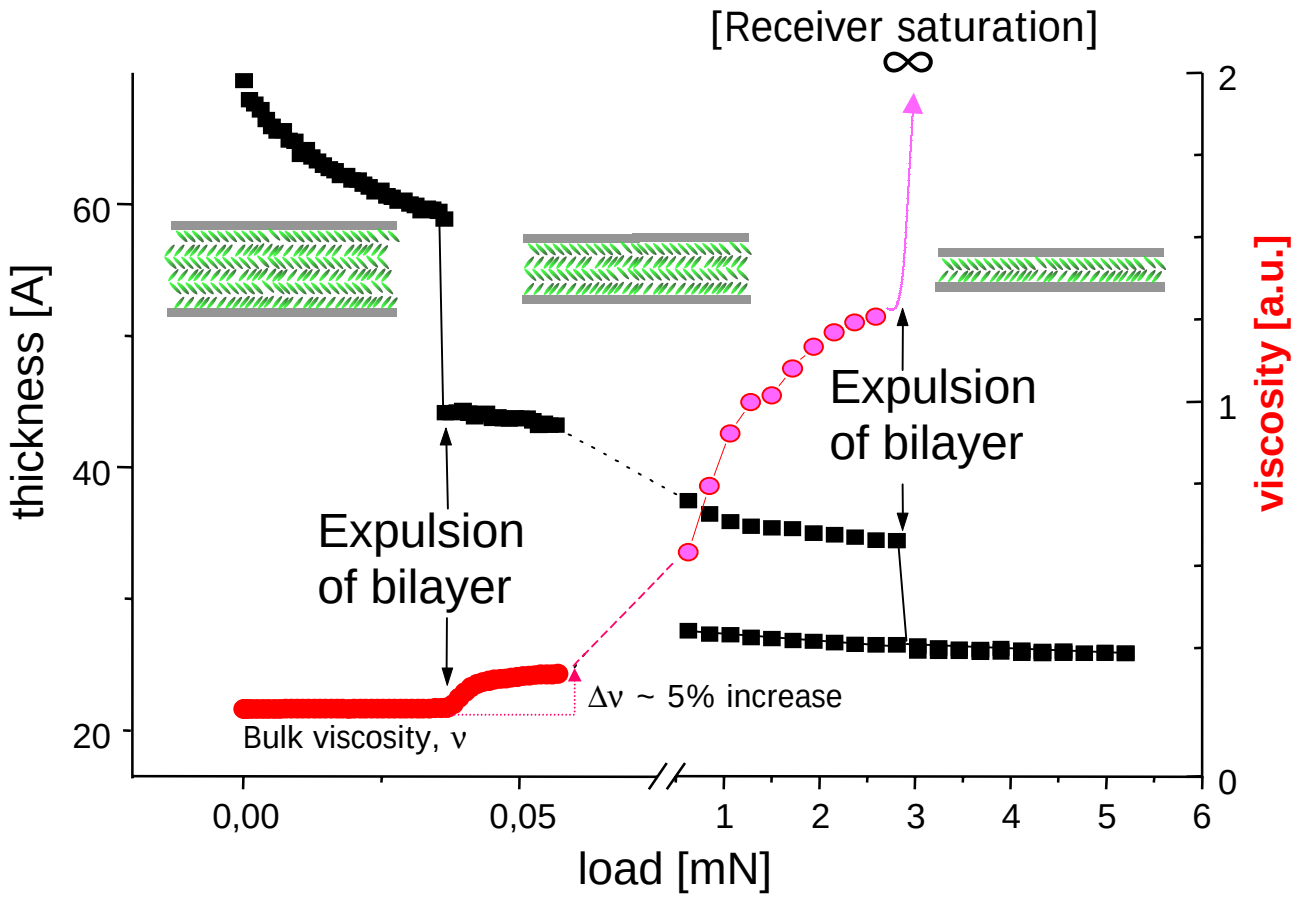

Stick-slip frictional behavior of the boundary monolayer

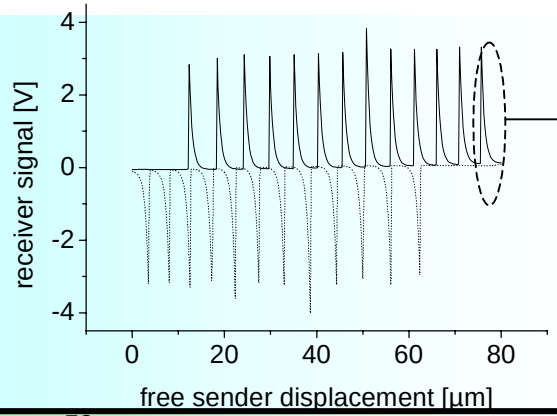

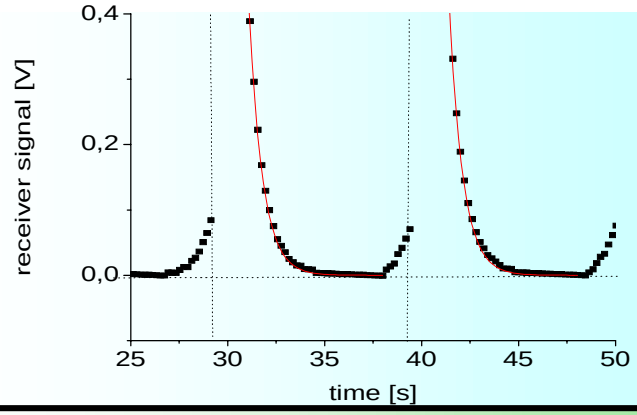

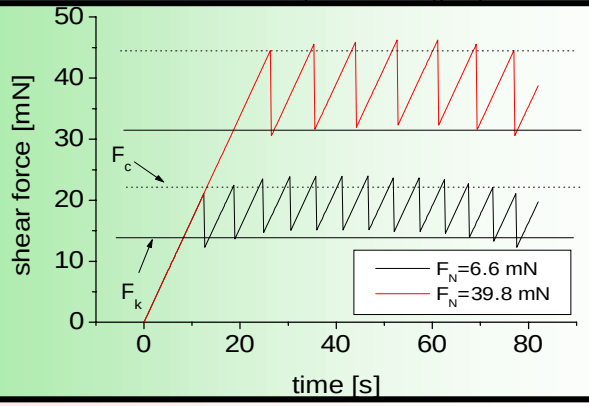

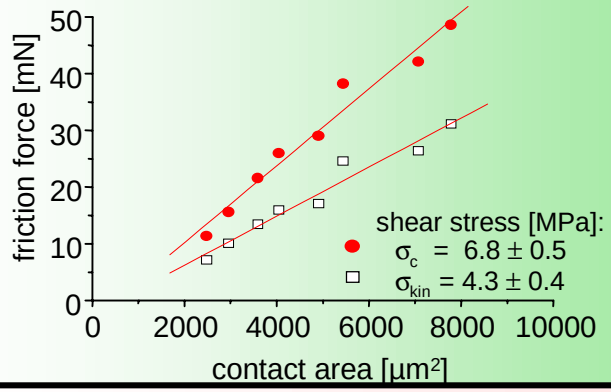

$$F_{spring}(t) = F_{static}^{max}.(1 - a.e^{-t/\tau_1} - b.e^{-t/\tau_2})$$

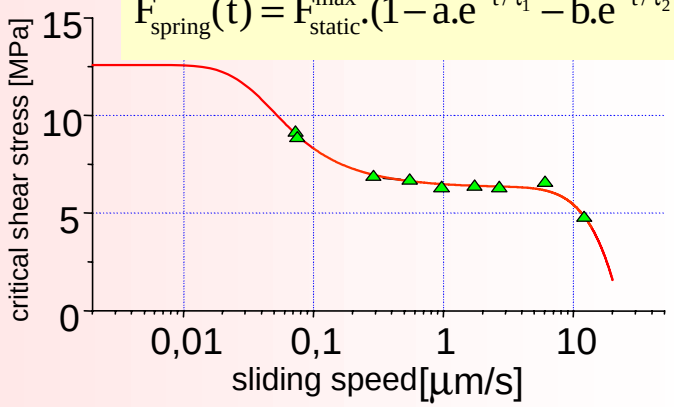

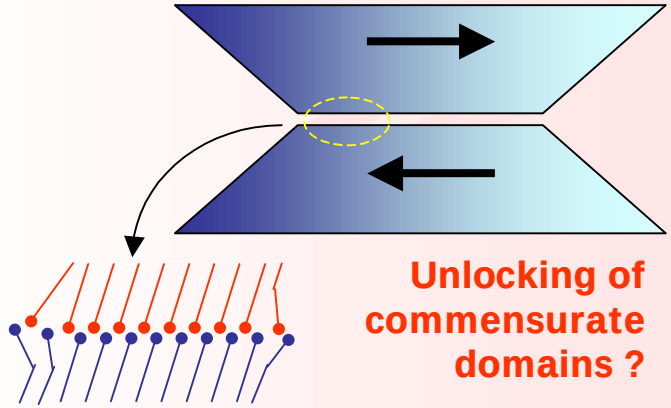

Unlocking of commensurate domains ?

Layering transitions in OMCTS

Slow approach:

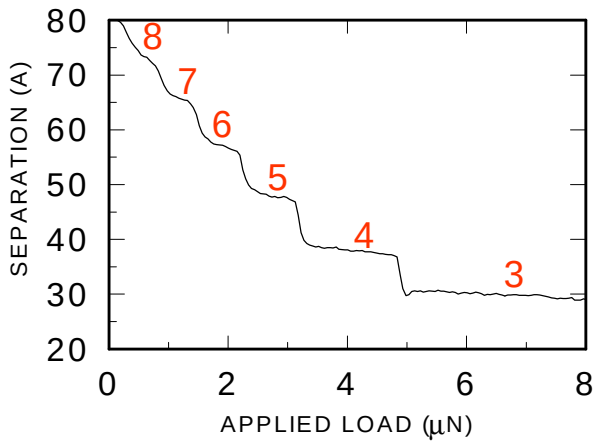

Fast approach: Data acquired in 1 s

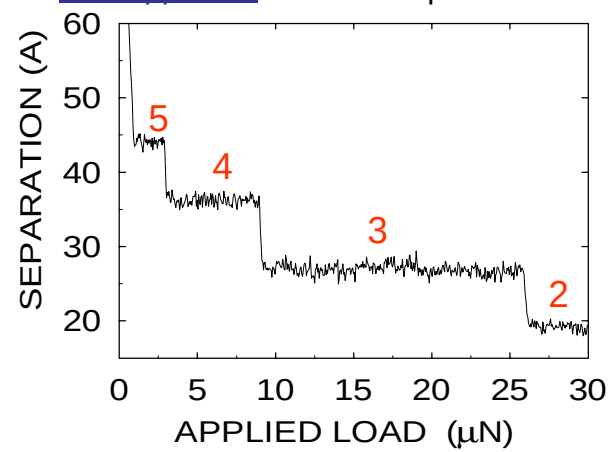

Fastest approach: $\Delta t \leq 1$ ms

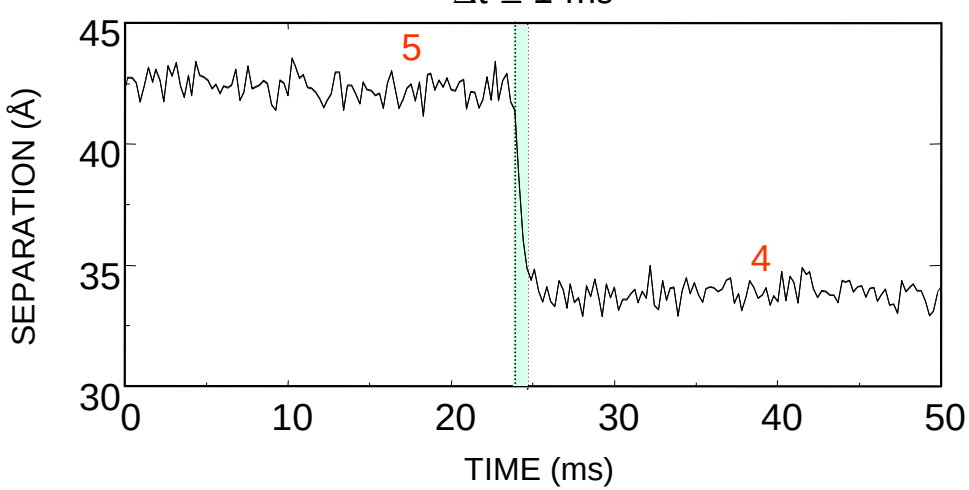

$$\Delta t = m n_a \eta A_0 / 4\pi h_0 P_{ext}$$

$$\eta \leq 10^{13}\ s^{-1}$$

These results show that the viscosity of layers 5=>4 (and others as well) is comparable to the bulk viscosity. Confinement does not increase it by orders of magnitude !

Lubrication of hard disks

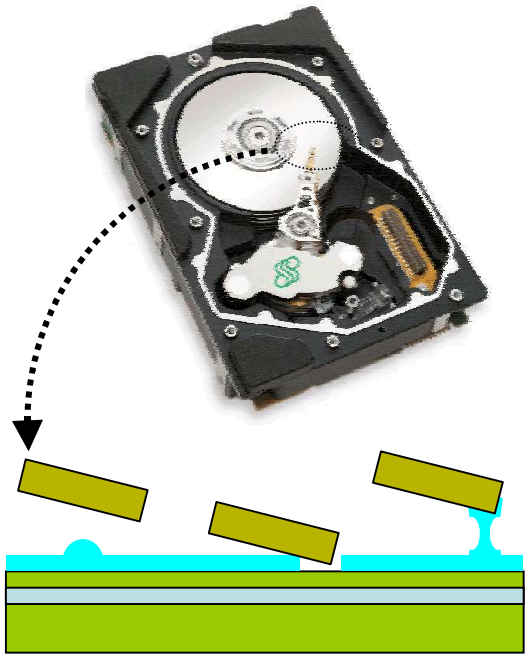

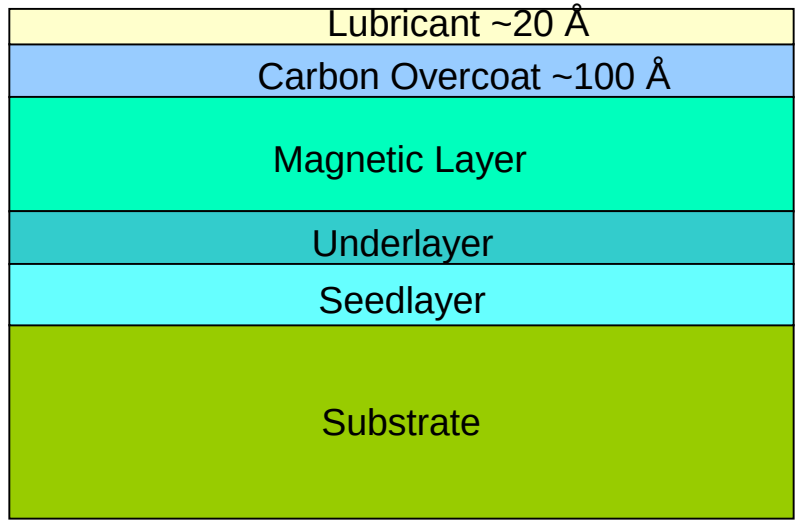

Perfluoropolyalkylethers (PFPE)

$$Y\text{-}\ (CF_2\text{-}CF_2\text{-}O)_m\text{-}(CF_2\text{-}O)_n\ \text{-}X$$

Zdol	X=Y= $-CH_2-OH$
Zdol-TX	X=Y= $-CH_2-O-CH_2-CH_2-O-CH_2-CH_2-OH$
Demnum	Y= CF_3; X= $-CH_2-OH$
Z03	X=Y= CF_3

Layering, mobility, de-wetting of Zdol-TX layers on a-carbon

SPFM images of liquid films of lubricant on hard disk

Electrostatic force moves 2nd layer but not 1st

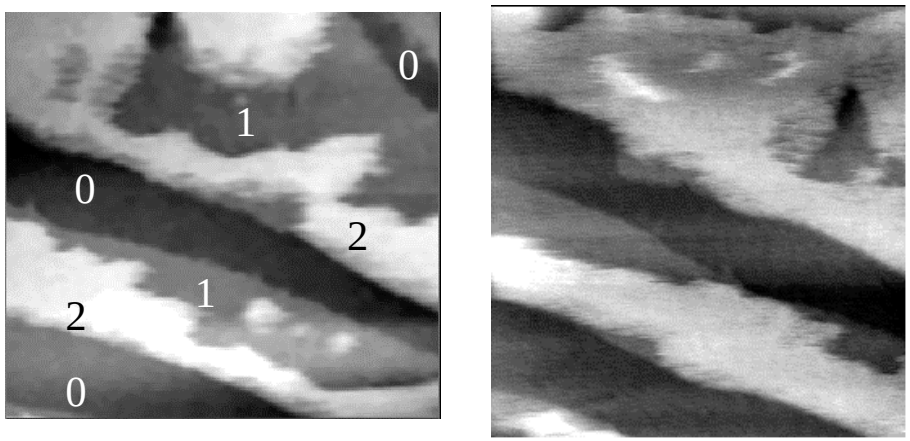

Contact moves both layers

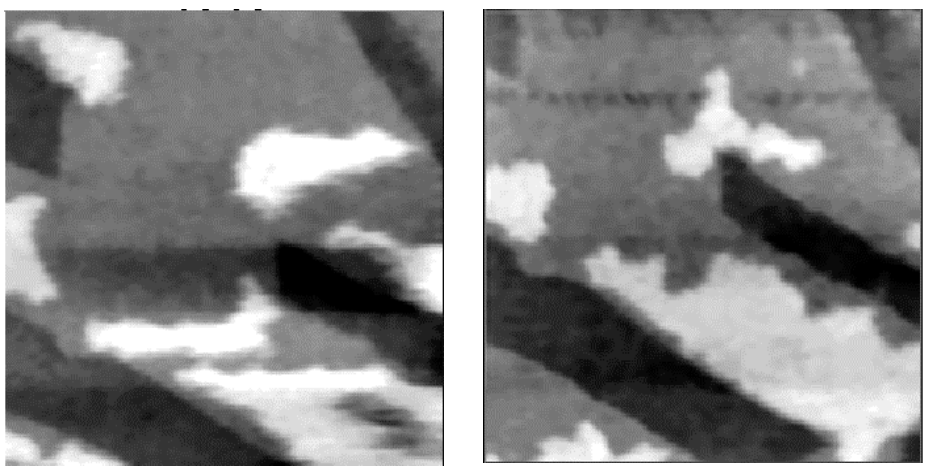

De-wetting: drop growth at the expense of 2nd layer

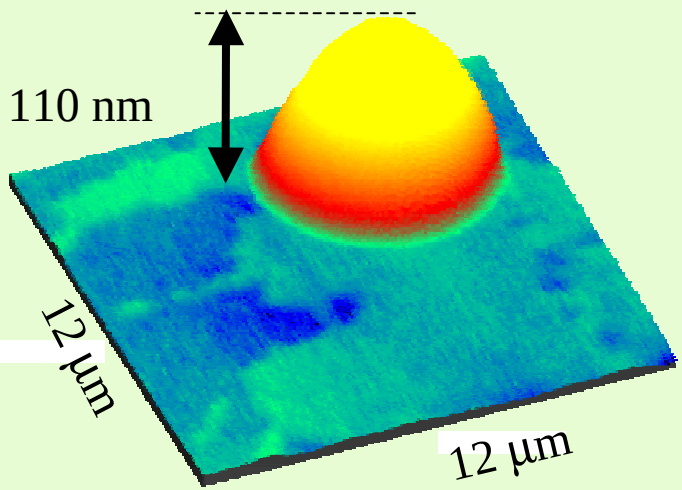

Dynamics of drainage

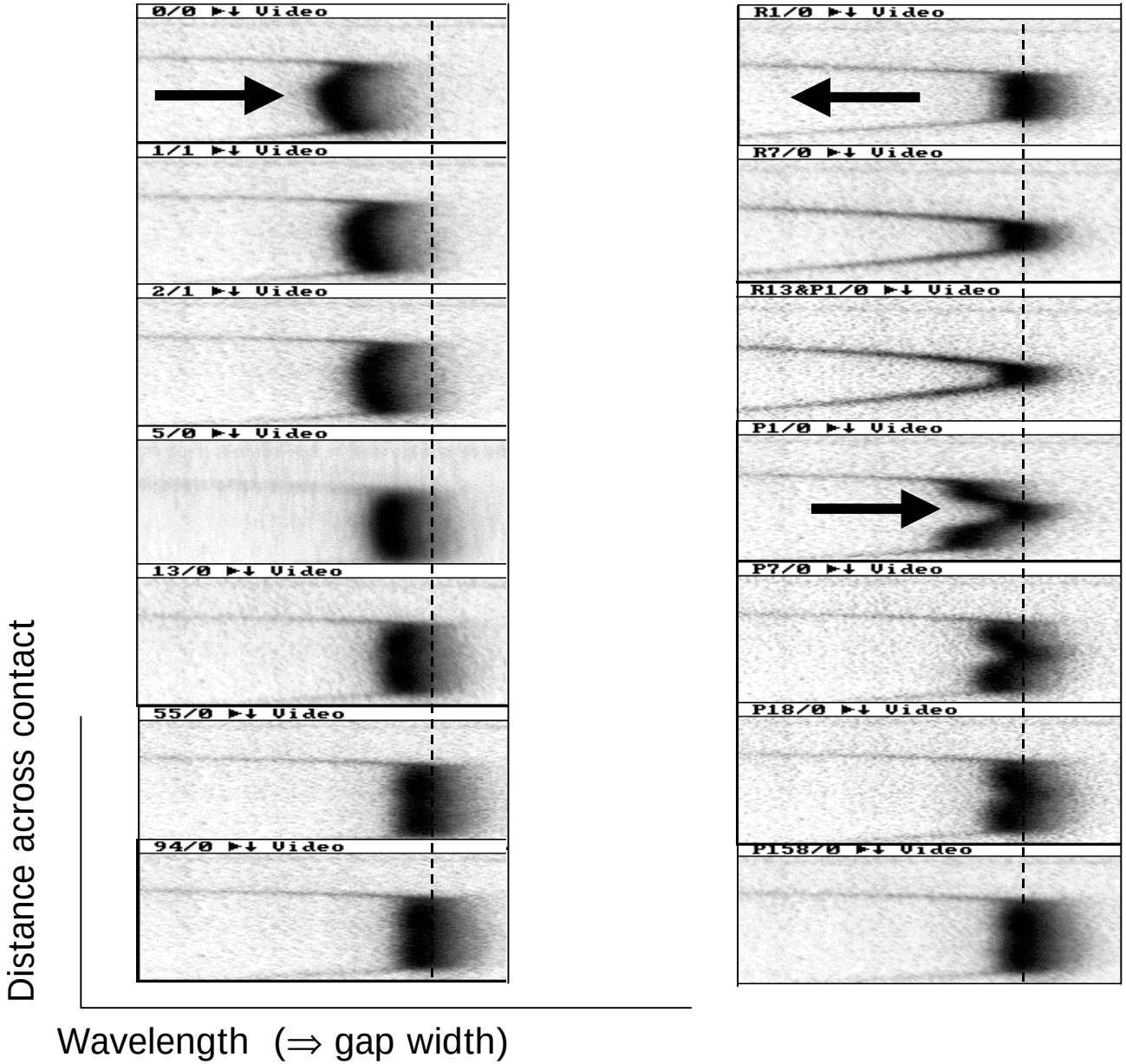

Drainage of Zdol and Demnum

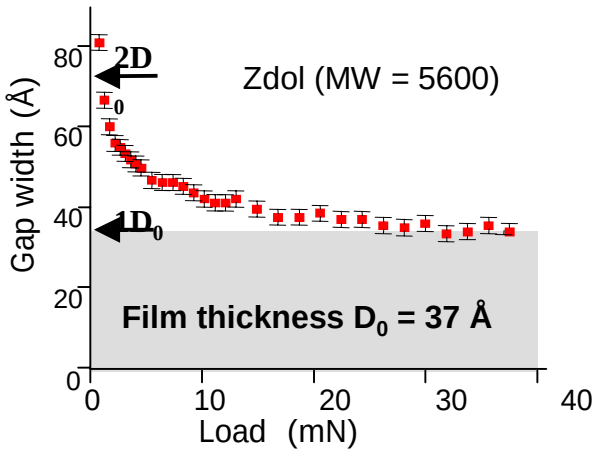

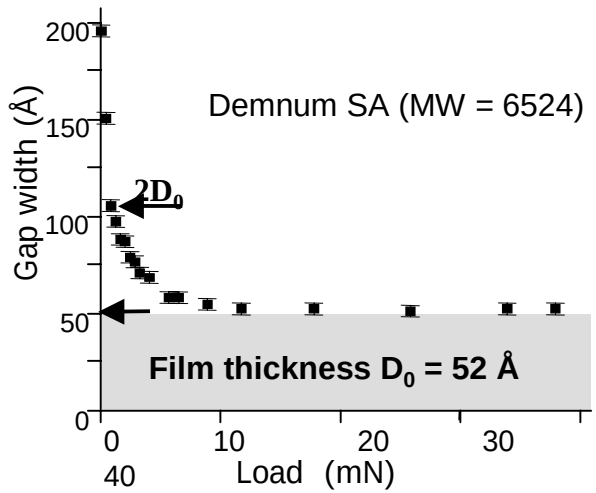

Thickness of the residual trapped layer

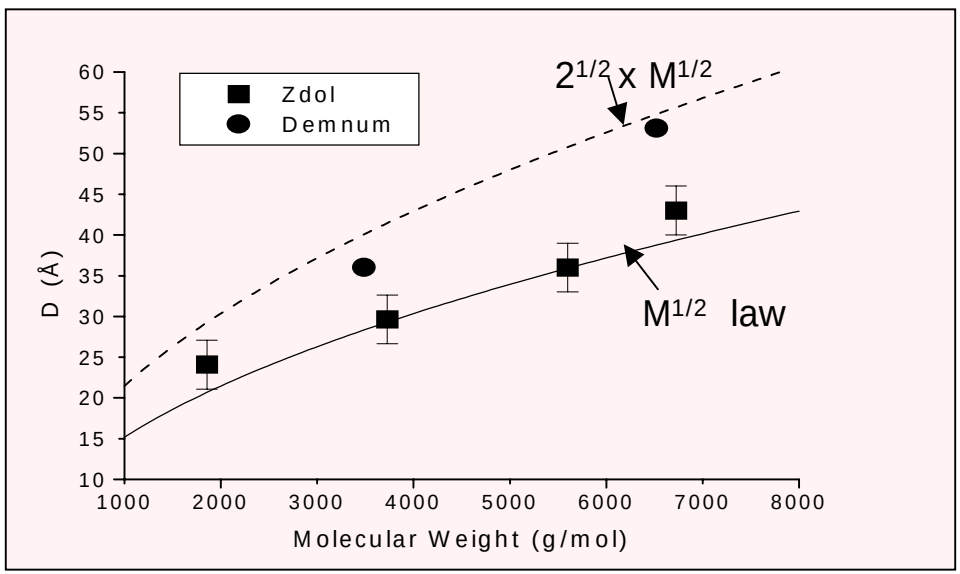

Dynamics of lubricant drainage

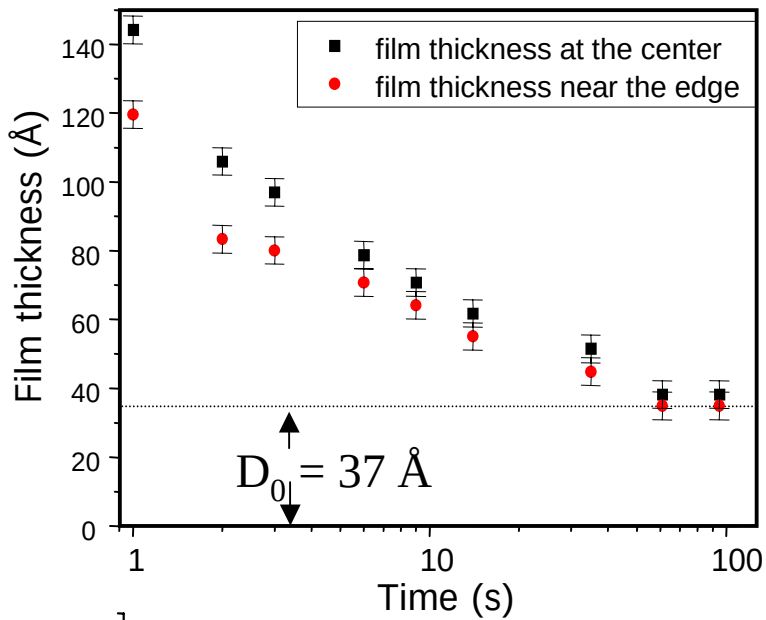

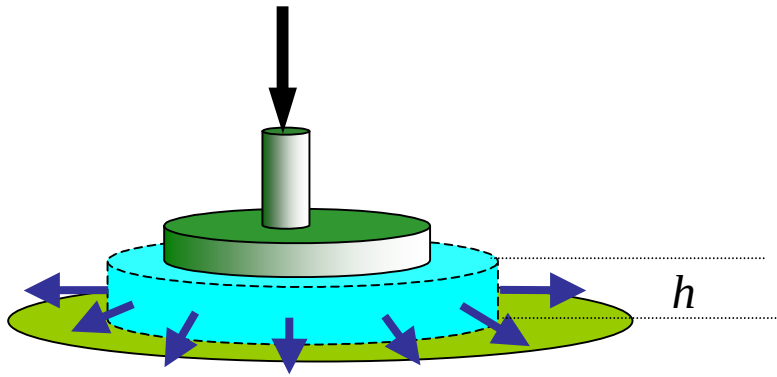

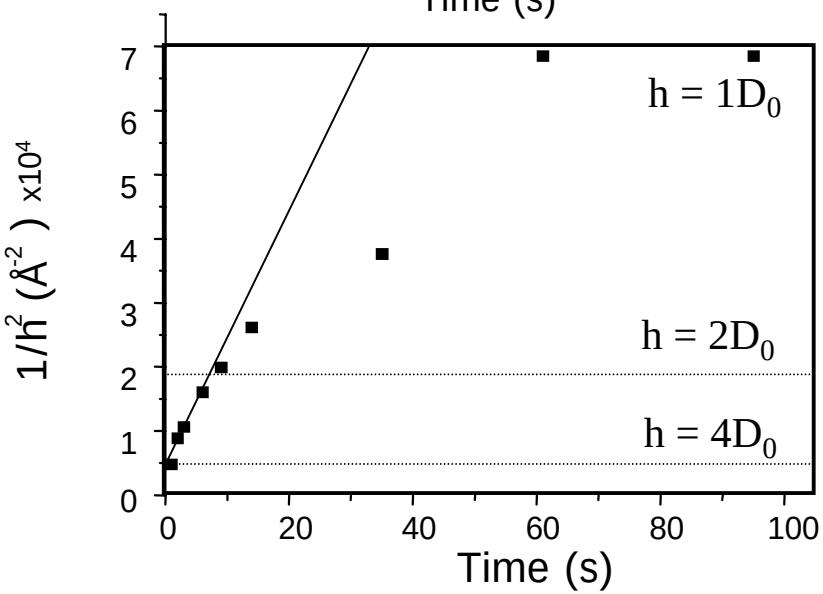

Navier-Stokes equation gives:

$$\frac{1}{h^2} = \frac{1}{h_o^2} + \frac{4Pt}{3\eta R^2}$$

Model:

$>4D_0$

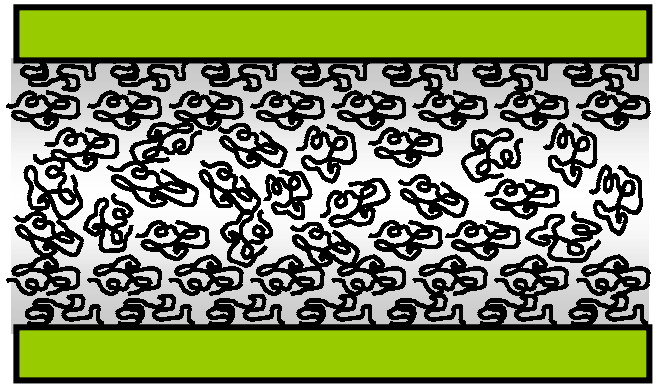

Bulk viscosity

η = 2 Poise

$4D_0$

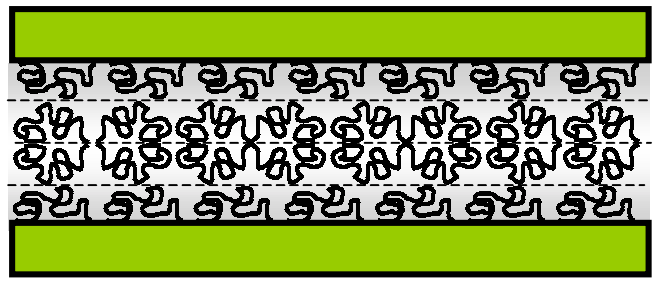

Enhanced viscosity

η > 20 Poise

$2D_0$

D_0